Reappraisal of Variscan tectonics in the southern French Massif Central

Dominique Chardon, Markus Aretz, Damien Roques

Reappraisal of Variscan tectonics in the southern French Massif Central

Dominique Chardon*, Markus Aretz and Damien Roques

GET, Université de Toulouse, CNRS, IRD, UPS, CNES, F-31400, France

Submitted to *Tectonophysics,* 22 February 2020

Revised 11 May 2020

*** Corresponding author**

Email: Dominique.chardon@ird.fr

Highlights

- Comprehensive review and kinematic reappraisal of nappe tectonics in the Southern Montagne Noire
- Nappes were thrust northeastwardly during flysch sedimentation in a sinistral transpressive context
- Implications for Variscan strike-slip tectonics before and during formation of the Iberian-Armorican syntax
- Implications for shear sense inversion and lower crust exhumation along long-lived transcurrent fault systems in orogens

Abstract

The comprehensive kinematic analysis of the Variscan fold nappes and associated wildflysch in the Southeastern Montagne Noire shows that the nappes were thrust northeastwardly along the Cévennes fault as a result of strike-slip-dominated sinistral transpression between 340 and 323 Ma. Macro- and map-scale recumbent folding and nappe stacking were achieved by ENE-directed, strike-parallel thrust shearing. The recumbent folds evolved into sheath folds by interplay of continued strike-parallel thrust shearing and strike-normal shortening manifested by north-verging folds that grew during wildflysch sedimentation. These results call for a tectonic reassessment of the southern side of the Variscides. The foreland basin was decoupled from the hinterland along orogen-scale sinistral fault(s) trending at a high angle to the orogenic trend, which interacted with a variety of hinterland-ward thrust systems. The shift from sinistral transpression to dextral transtension along the Cévennes fault after 317 Ma accompanied the closure of the Iberian-Armorican syntax by accommodating northeastward escape and

gravitational collapse of the northern limb of the syntax. These results illustrate the shift from plate convergence-controlled to escape-controlled kinematics on shear sense reversal and lower crust exhumation along long-lived strike-slip fault systems.

Keywords: Nappe tectonics, Sheath fold, Transpression, Wildflysch, Montagne Noire, Cévennes fault, Iberian-Armorican syntax

1. Introduction

Lateral movements in collisional orogens are assisted by continental-scale transcurrent fault systems and accompanied by extension of the hot thickened crust. These displacements respond to continental indentation, the formation of syntaxes (i.e., bends in orogens) and/or the creation of a favorable boundary condition for escape. Such processes have significantly distorted the collisional structural pattern of the Variscides (Burg et al., 1994; Martínez-Catalán, 2011), as exemplified around the Iberian-Armorican syntax (Fig. 1a). Despite that distortion, the geotraverse of the Southern Variscides through the Eastern French Massif Central (Fig. 1a) has long been interpreted in terms of southward growth of the collisional prism at the expense of the foreland basin (e.g., Matte, 2007). At the southern end of that geotraverse, the Montagne Noire (Fig. 1) is a type locality at the hinterland-foreland transition where outward orogen-normal thrusting during flysch sedimentation is classically postulated (Matte, 1983, 2007; Franke and Engel, 1986; Soula et al., 2001; Malavieille, 2010).

The Montagne Noire exposes a gneiss dome (or "Axial Zone") mantled by Paleozoic series folded together with the Visean – Serpukovian Kulm flysch sediments of the foreland basin (Engel, 1984; Fig. 1). In the southern flank of the dome, Bergeron (1904) first suggested

63 the occurrence of thrust nappes, for which Von Gaertner (1937a, 1937b) introduced the analogy
64 with the Helvetic nappes of Switzerland (e.g., Ramsay et al., 1983) i.e., the nappes originated in
65 the northern flank of the dome and were extruded southward. The impressive work of Gèze
66 (1949) established the recumbent fold structure of the nappes, which he interpreted to result from
67 north-vergent thrusting against the dome. In an exemplary fair play controversy published in a
68 common paper with Gèze (Gèze et al., 1952), de Sitter and Trümpy relaunched the Helvetic
69 analogy through a clever model of southward nappe emplacement. The 60' saw the advent of
70 kinematic analysis of bedding / cleavage / fold asymmetry relationships in the Montagne Noire
71 (Rodgers, 1962; Mattauer and Proust, 1963). That approach led to a model of south-verging fold
72 nappes (Arthaud et al., 1966; Arthaud, 1970), which was later coupled to a tectonosedimentary
73 model linking wildflysch sedimentation to southward nappe propagation (Engel et al., 1978).
74 Several attempts were made at deciphering deformation of the Axial Zone, where pre-
75 doming fabrics are inferred to have formed during thrust nappe tectonics (e.g., Ellenberger,
76 1967; Van Den Driessche and Brun, 1992; Demange, 1998; Soula et al., 2001; Charles et al.,
77 2009). But the Axial zone and its southern envelop lack N-S shearing features. They are affected
78 by pervasive ENE stretching and strike-slip deformation (Nicolas et al., 1977; Beaud, 1985;
79 Faure and Cottereau, 1988; Echtler and Malavieille, 1990; Aerden, 1998; Matte et al., 1998;
80 Schranzhofer, 1999; Franke et al., 2011; Rabin et al., 2015). This, together with perceptive
81 criticisms of the nappe kinematic model (Collomb and Ellenberger, 1965; Ellenberger, 1980; Lee
82 et al., 1988) did not however lead to question the southward nappe emplacement paradigm.
83 In the present paper, we provide a critical review pointing to the disputable kinematics of
84 the southward nappe emplacement model and recalling its paleogeographic inconsistencies. We
85 then present the first comprehensive structural and kinematic analysis of the nappes in the

86 southeastern Montagne Noire integrating deformation of the wildflysch. We show that the
87 nappes were thrust northeastwardly during wildflysch sedimentation in a sinistral transpressional
88 context. This result calls for a revision of the convergent deformation scheme of the southern
89 Variscan foreland, with a preponderant role of orogen-scale transcurrent faulting before and
90 during amplification of the Iberian-Armorican syntax.
91
92 **2. Geological outline**
93 The study area comprises the easternmost part of the Pardailhan unit and the underlying terrains
94 located to the East (i.e., the Mont Peyroux, Faugères and Cabrières nappes of Arthaud, 1970;
95 Figs. 1b and 2). The nappes are supported by the schistose envelope of the Axial zone (the so-
96 called Schistes X of Ediacarian to Early Cambrian age), which constitutes a mid-crustal
97 décollement. The stratigraphic succession consists of Schistes X, Ordovician pelitic schists,
98 Devonian-Tournaisian carbonate and chert series, and the Mississippian Kulm flysch grading
99 upward into a wildflysch (Engel et al., 1978; Aretz, 2016; Fig. 2). The so-called Écailles de
100 Cabrières are mostly slabs or slivers (*écailles* in French) of Ordovician to lower Carboniferous
101 series transported upon the wildflysch (Gèze, 1949). The regional structure is marked by map-
102 scale folds trending ENE in the western part of the map area (Figs. 2, 3a and 3b). These folds
103 (referred to as F_2 in the present work) are inclined to slightly overturned northward and have
104 been documented at various scales throughout the study area (e.g., Lee, 1988) and considered as
105 post-nappe. The Pardailhan unit essentially consists in the lower limb of a ENE-trending and
106 slightly S-dipping, faulted and refolded recumbent anticline cored by massive Cambrian
107 sedimentary series (Gèze, 1949; Echtler, 1990).
108

3. Origin and kinematics of the nappes: old pending issues

Bedding / cleavage / fold asymmetry relationships that would be indicative of southward recumbent folding are actually restricted to portions of the Pardailhan nappe (Arthaud, 1970). But even in this unit, the north-facing folds affecting the inverted series have been shown to be F_2 folds documented in both normal and overturned limbs of the nappes (Lee, 1988; see also Cassard et al., 1993) instead of second-order folds that would typify the overturned limb of a south-verging fold nappe (see Rodgers, 1962). The pervasive ENE-trending stretching lineation affecting the nappes was originally interpreted as B-type i.e., parallel to the axes of the south-verging recumbent folds (Arthaud, 1969). This lineation is however pervasive in the dome too and parallel to the F2 folds, which led Collomb and Ellenberger (1965) to challenge N-S nappe emplacement kinematics deduced from the schistosity bearing that lineation. Besides, the development of overturned fold limbs several kilometers wide was not readily reconciled with stretching parallel to the recumbent fold axes and normal to a N-S nappe displacement direction (discussions in Burg and Matte, 1978; Harris et al., 1983; Matte, 1983; Echtler, 1990). ENE stretching in the Mont Peyroux nappe and Western Faugères nappe (Figs 1b and 2) was later to be shown to record eastward shearing (Lee, 1988; Lee et al., 1988). These authors also first documented top-to the-S shear criteria in the upper (southern) part of the Pardailhan unit that they interpreted as due to gravitational gliding. Echtler (1990) related these shears to post-recumbent folding, late orogenic extensional detachment faults coeval with dome emplacement. To reconcile southward gliding and ENE stretching, Aerden and Malavieille (1999) conceived a model combining coeval, syn-convergence southward collapse of the orogenic front - forming the recumbent folds - and N-S shortening producing the ENE F_2 folds and stretching. But these authors seem to have overlooked eastward shearing, as did Mattauer et al. (1996), who pleaded

for post-nappe ENE coaxial stretching. More recently, Wiederer et al. (2002) and Franke et al. (2011) interpreted top-to-the ENE shearing at the contact between the Mont Peyroux and Faugères nappes (Fig. 2) as indicative of an extensional detachment folded by the regional F_2 folds. Their model takes up that of Echtler and Malavieille (1990), in which the dome emplaced in a dextral transtensional releasing bend ("pull apart") of the Cévennes fault (Fig. 1b) but with superimposed N-S shortening to account for ENE F_2 folding. However, top-to the ENE shearing and N-S shortening are not compatible with dextral slip along the dome's flank; it would instead require sinistral shearing. Furthermore, the subtractive break expected across such an extensional detachment at the Mont Peyroux – Faugères contact is not documented in the regional pattern of very low-grade metamorphism (Franke et al., 2011; Doublier al., 2015). By emphasizing post-nappe deformation in the Mont Peyroux and Faugères units, Franke et al. (2011) came to argue that no markers of original southward nappe emplacement remained but the overturned series. This would again not be reconcilable with the strain expected to account for the amplitude of the overturned fold limbs. Finally, it is noteworthy that the Montagne Noire south-vergent fold-and-thrust model as extended by Arthaud et al. (1976) up to the Mouthoumet massif (Fig. 1b) shows no thrust emerging with a northern dip. All the thrusts would indeed be S-dipping and mostly cushioned in the flysch, casting further doubt on the south-verging thrusting model.

From paleogeographic and stratigraphic viewpoints, no evidence supports a northern origin for the nappes either (Ellenberger, 1980). Even promoters of the southward nappe emplacement model acknowledged that paleogeography does not provide a decisive test of a northern or a southern origin for the nappes (see Gèze et al., 1952; Arthaud, 1970). Besides, Devonian series and the Carboniferous flysch are not present in the northern thrust belt, but only in the southern flank of the Montagne Noire, in the Mouthoumet Massif and in the Pyrenees (Fig.

155 1b). Moreover, the Lower Paleozoic of the Écailles de Cabrières has long been known to have
156 clear affinities with that of the Mouthoumet massif and the Pyrenees and not with the rest of the
157 Montagne Noire or the Massif Central (Engel et al., 1978; Fig. 1b). The interpretation of the
158 Écailles de Cabrières as miniature nappes derived from southward propagating fold nappes in the
159 Montagne Noire (De Sitter and Trümpy *in* Gèze et al., 1952; Engel et al., 1978, 1981; Vachard et
160 al., 2017) is therefore untenable.
161
162 **4. Structural and kinematic analysis**
163 ***4. 1. Overall structure***
164 Our investigations led to a structural scheme that does not require a distinction between a Mont
165 Peyroux and a Faugères nappe (Fig. 2). The Mont Peyroux overturned series and the Mont de
166 Faugères normal series are simply part of a regional-scale, recumbent F_1 east-verging recumbent
167 syncline with an axis initially trending close to N-S, which has been refolded by the map-scale F_2
168 ENE trending folds (Figs. 2, 3a and 3b). That syncline is called hereafter the Orb syncline, for its
169 axial trace follows the Orb River for some distance SW of Le Lau (Figs. 3a and 4a). Both limbs
170 of the F_1 Orb syncline are attenuated northward as F_2 folds become tighter (Figs. 3b and 4a). The
171 wildflysch belongs to the normal forelimb of the Orb syncline and is bounded to the North by the
172 Roquessels fault (Engel et al., 1978, 1981; Fig. 2). The Orb syncline tectonically overlies in the
173 North parautochtonous units detached from the Schistes X and is overlain to the West by the
174 Pardailhan unit and to the East and Southeast by the Pic the Vissou and Écailles de Cabrières
175 units (Figs. 2 and 4a). The parautochtonous units and Schistes X form a corridor of steeper and
176 more penetrative schistosity or foliation concordant with the gneissic fabric of the dome. That
177 northern fringe of the study area is called hereafter the northern deformation belt (Fig. 4a).

Given the late exhumation of the gneissic lower crust along the northern deformation belt and the southeastward decreasing very low-grade metamorphism in the nappes (Engel et al., 1981; Wiederer et al., 2002; Franke et al., 2011; Doublier et al., 2015), the map in Figure 2 also provides a kind of cross sectional view of the upper crust, with progressively shallower levels exposed in the south. The present work relies on extensive structural mapping based on more than 700 field stations dedicated to structural measurements, kinematic observations and logging of roadside sections.

4. 2. Deep Upper Crust

This crustal level comprises the terrains located NNW of the Roquessels fault and Roquebrun, and West of Cabrières (Fig. 2). The area is affected by a regional, penetrative schistosity or slaty cleavage and locally by a fracture cleavage in massive sandstones collectively called $S_{1\text{-}2}$ (Figs. 4c and 6a). This planar fabric bears a ubiquitous, NNE- to NE-trending, shallowly plunging stretching lineation (Figs. 3c and 5b) marked by quartz fibers or the elongation of quartz aggregates in siliciclatics and by calcite fibers and the elongation of nodules in carbonates ($L_{1\text{-}2}$).

4. 2. 1. Monts de Faugères

The Monts de Faugères East of 3°05'E (Fig. 2) consist in a north-facing recumbent anticlinal fold sheet of Devonian carbonates with its backlimb supporting the flysch (Fig. 4c to 4e). The schistosity of the backlimb is moderately to shallowly south dipping (Fig. 5a). The structure of the backlimb Devonian limestones may be complex in details, as exemplified by second-order, northwardly inclined to slightly overturned F_2 folds (the regional $S_{1\text{-}2}$ schistosity being axial planar to those folds) and stratigraphic repetitions (Maurel, 1966; Pinna and Prunac, 1976;

Mattauer et al., 1996). But the structural envelop of the Devonian remains shallowly South dipping and local fault/fold patterns are systematically indicative of South-over-North apparent thrusting / vergence (Maurel, 1966; Pinna and Prunac, 1976; present work; Fig. 4). Planar and linear D_{1-2} fabrics in the flysch are associated with pervasive top-to-the ENE shearing recorded by pervasive shallowly dipping shear zones (Figs. 5c). Shearing parallel to the regional stretching lineation and the recumbent fold axes as well as the common attenuation of the fold limbs along the shear zones attests to a genetic link between recumbent folding and shearing (Figs. 6a and 6b). The occurrence of macroscopic sheath folds (Fig. 6c) further attests to the intensity of the simple shear component of deformation (Cobbold and Quinquis, 1980). Intense LS tectonites affect the carbonates (Fig. 6d) but recrystallization into marble seems to have prevented preservation of macroscopic shear criteria. Microscopic shear criteria (Lee, 1988) and calcite lattice preferential orientation (Mattauer et al., 1996) are however indicative of top-to-the ENE shearing too. West of Cabrières, the eastern termination of the Devonian limestones corresponds to the nose of a sheath anticline that would be compatible with the regional ENE shearing regime documented throughout the Monts de Faugères (e.g., Figs. 4 and 6). Schistosity trajectories in the Monts de Faugères (Fig. 5a) delineate a series of shallowly SSE-dipping shear zones that are interpreted to have accompanied differential top-to-the ENE shearing (Fig. 5c).

The parautochtonous units display a fabric map pattern comparable to that of the overlying Monts de Faugères fold sheet although with higher dips of the planar fabric that becomes in most cases a foliation (Figs. 4b to 4d; Fig. 5). Top-to-the NE shearing is documented at the base of the Mont de Faugères fold sheet (e.g., Fig. 5c), suggesting partitioning between internal top-to-the ENE shearing deformation in the fold sheet and top-to-the NE slip at its base / northern margin. Top-to-the NE sense of shear is documented as well within and at the base of

224 the para autochtonous units (Fig. 5c). A tectonic window exposing the flysch in the Monts de
225 Faugères (Fig. 2) implies at least several km of transport of the fold sheet towards the ENE / NE
226 (Figs. 4d and 4e). To summarize, the structure, internal deformation and kinematics of the Monts
227 de Faugères fold sheet and the underlying parautochthonous units are indicative of a ENE- to
228 NE-vergent, sinistral transpressive low-angle thrust system (Fig. 4).
229
230 *4. 2. 2. Western Monts de Faugères and the rest of the deep upper crust*
231 The western termination of the Monts de Faugères Devonian corresponds to the F_2 Le Lau
232 antiform (Figs. 2 3b and 4a). The hinge of the antiform is affected by a beam of NE-trending
233 second-order folds parallel to the regional stretching lineation (Figs. 3a and 5b). These folds have
234 no systematic asymmetry and /or complex N-S cross-sectional geometries (Arthaud, 1964) that
235 are actually mostly those of sheath folds (Franke et al., 2011). Deformation in the fold beam is
236 associated with top-to-the ENE to NE sense of shear parallel to the regional stretching lineation
237 (Fig. 5c). This shearing pattern - but devoid of sheath folds - also affects the overturned Mont
238 Peyroux limb further to the West (Fig. 6d) and is richly documented upward (westward) in the
239 structural pile, including the Pardailhan unit (Fig. 5c). Map-scale shear zones laminating the
240 inverted Mont Peyroux limb are interpreted as recording localization of regional top-to-the ENE
241 shearing (Figs. 2, 4a and 4b). The regional schistosity wraps the Le Lau antiform, together with
242 the overturned Mont Peyroux limb and its sub concordant shear zones (Figs. 4a and 5a).
243 The Laurenque F_2 synform affects the flysch between Roquebrun and Le Lau (Figs. 2, 3b
244 and 4a). The fold refolds the axial plane of the F1 Orb syncline but the map axial trace of the F1
245 fold may not be mapped precisely (Figs. 3a and 3b). The Laurenque fold is interpreted as a
246 sheath fold with its nose pointing to the ENE. Shallowly S-dipping $S_{1\text{-}2}$ appears to be axial-planar

247 to that fold, which has undergone pervasive ENE-directed shearing and generated a schistosity
248 triple point at its eastern termination (Figs. 2 and 5). This indicates fold growth – most probably
249 by eastward shearing - during NNW-directed shortening.
250 The Le Lau antiform is followed to the North by the map-scale F_2 l'Aire Marty syncline
251 refolding the F_1 Orb syncline and the shear zones of its overturned and normal limbs (Figs. 3 and
252 4a). The northern limb of that F_2 fold is attenuated and taken into the northern deformation belt
253 (Figs. 5 and 4a). Top-to the ENE / sinistral shearing, comparable to that documented in the
254 allochtonous units, prevails throughout the northern deformation belt (Figs. 5c and 4a; see also
255 Beaud, 1985; Lee, 1988; Schranzhofer, 1999).
256 To summarize, eastward shearing affecting the normal limb of the F_1 Orb syncline
257 (Monts de Faugères) is also pervasive in its western overturned limb (Mont Peyroux) and the
258 overlying Pardailhan unit. Eastward shearing is interpreted to have overturned the Mont Peyroux
259 limb and Pardailhan series and thrust the Pardailhan unit over the Mont Peyroux inverted
260 backlimb of the F_1 Orb syncline. Eastward shearing produced shear-parallel sheath folds that are
261 also parallel to F_2 folds formed by NNW shortening, in agreement with low-angle sinistral
262 transpressional thrusting documented in the Monts de Faugères and overlying flysch, the
263 parautochthonous units and the northern deformation belt.
264
265 ***4. 3. Uppermost Crust: Wildflysch and Écailles de Cabrières***
266 Along the cross-section of Figure 4b, the Mont Peyroux overturned fold limb exposes a
267 continuous stratigraphy from the Devonian to the wildflysch. The eastward transition from
268 overturned to normal bedding along that section (Engel et al., 1981) is interpreted as a
269 progressive unconformity formed by eastward overturning of the Mont Peyroux limb. Higher up

(eastward; Fig. 2) in the wildflysch stratigraphy, at least two main unconformities are documented (Fig. S1, supplementary material). They are deformed by map-scale F_2 folds (Figs. 2, 3a and 4c). The oldest of the two unconformities passes by Lenthéric (Fig. 4b) and is taken into the steep overturned forelimb of a F_2 anticline (Figs. 4c and 4d). Downlaps on this unconformity (Fig. 4d) indicate northeastward progradation of the wildflysch. The youngest unconformity is a progressive unconformity passing by Laurens and La Plaine (Figs. 2 and 4c) that shows a northward-fanning pattern of bedding indicative of north- or northeastward progradation / thickening of the flysch sequence. Northeastward progradation of the flysch series is consistent with syn-sedimentary NE-vergent F_2 folding and thrusting (Figs. 2 and 4).

The basal (western) contact of the Écailles de Cabrières unit is sub horizontal and truncates the underlying folded flysch sequence described above (Figs. 2 and 4d). The Écailles de Cabrières unit is made of duplex lenses separated by low-angle S-dipping faults, most of which root into the basal contact (Figs. 4d to 4f). The South-over-North stacking pattern of the lenses (Figs. 4d to 4f) revealed by the detailed investigations of Gèze (1949) and Maurel (1966) is consistent with the top-to-the NE to ENE reverse shear criteria we collected along the basal contact, along the internal contacts and within the flysch of the Écailles de Cabrières unit (Figs. 4, 5c, 7, 8a and 8c). The Écailles de Cabrières unit is interpreted as a shallow NE-vergent thrust system having propagated over the folded flysch basin (e.g., Figs. 2 and 4d), in agreement with North-vergent thrust folding and the unconformity patterns in the underlying wildflysch basin.

The Roquessels mass transport complex (Fig. 2) is made of a mix of pre- and syn-flysch lithologies stacked at the northwestern front of the Écailles de Cabrières unit (Fig. 4d). Low angle, top-to the WSW shearing affects the eastern portion of the mass transport complex (Fig. 8b), whereas syn-sedimentary (syn-flysch), top to the WSW normal faulting and gliding is

293 documented near the western termination of the mass transport complex (Fig. 8c). The latter
294 pattern may result from westward gravitational escape of the mass transport complex at the front
295 of the northeastward propagating Écailles de Cabrières unit. The former pattern may either be
296 related to (1) lateral escape process recorded at a lower (i.e., solid-state / ductile) structural level
297 of the glided mass or (2) early, low angle westward detachment faulting prefiguring the
298 Roquessels fault (see section 4.4).
299 Relatively low penetrative deformation of the Écailles de Cabrières unit allows for the
300 preservation of syn-sedimentary gliding and normal faulting features within or at the base of reef
301 carbonate massifs in the flysch series (Fig. S2, supplementary material). Senses of slip on the
302 gliding surfaces and normal faults are mostly top-to-the South and, to a lesser extent, top-to the
303 WSW (Fig. 5c).
304
305 ***4. 4. Late Dextral Transtensional Fault System***
306 Normal-dextral kinematics of the Roquessels fault (Engel et al., 1981) are attested to by fractures
307 in massive vein quartz injected in the fault (Figs. 2 and 4), with a mean pitch of 60° to the WSW
308 (e.g., Vailhan dam; Fig. 2). The normal component of slip on the fault is consistent with a
309 subtractive break in the very-low grade metamorphic map pattern (Engel et al., 1981) and the
310 more penetrative schistosity affecting the flysch in its footwall than in its hangingwall.
311 Documentation of low-angle, top-to-the WSW shear criteria in the vicinity of the Roquessels
312 fault (Figs. 5c and 8b) suggests that the fault recorded late (C' type) brittle strain localization
313 across an earlier, lower angle detachment (Engel et al., 1981 had a comparable interpretation of
314 strain localization, but in the hypothesis of a south-verging and south-dipping early Roquessels
315 thrust fault). The Roquessels fault connects westward with the shear zone ramp mapped North of

316 Roquebrun that roots into the deep overturned Mont Peyroux limb (Figs. 2, 4b and 5c),
317 indicating that the Roquessels fault is a reactivated thrust ramp. The Roquessels fault extends
318 further to the West to crosscut the basal contact of the Pardailhan unit (Figs 2 and 5c). South
319 dipping faults with top-to-the SW and SSW (i.e., dextral-transtensional) slip are documented in
320 the Pardailhan unit, especially south of the western extension of the Roquessels fault (Lee, 1988;
321 Echtler, 1990). Those faults reactivate ramps associated with F_2 north-vergent anticlines (Lee,
322 1988).
323 NW of Cabrières, the basal contact of the Écailles de Cabrières and Pic de Vissou units
324 over the Mont de Faugères series (Figs. 2 and 4f) marks a subtractive metamorphic break
325 indicative of extensional décollement shearing after emplacement of those units (Engel et al.,
326 1981). Top-to the WSW shearing with syn-kinematic emplacement of massive quartz veins
327 along this décollement appears to post-date eastward shearing in the Monts de Faugères and the
328 Écailles de Cabrières unit (Fig. 5c). The décollement is interpreted to have accompanied top-to-
329 the WSW dextral transtension along the Roquessels fault system. Localized top-to the W or SW
330 (i.e., dextral) shearing is also documented along shear zones - often associated with quartz veins
331 – in the northern deformation zone where top-to-the ENE shearing features are dominant (Figs.
332 4d, 4e and 5c; see also Lee, 1988 and Schranzhofer, 1999). Likewise, dextral top-to-the WSW
333 shearing is documented along the basal contact of the Mont Peyroux-Monts de Faugères series
334 West of 3°05'E as well as along the Le Lau fault (Figs. 5c). Dextral shears are also documented
335 further to the West in the northern deformation belt and along the basal contact of the Pardailhan
336 and Minervois nappes (Echtler, 1990; Cassard et al., 1993; Fig. 1b).
337
338 **5. Interpretation**

5. 1. Early Left-Lateral Transpressional Fold-and-Thrust Tectonics

The strain pattern of the southeastern Montagne Noire formed by the interplay of (1) pervasive top-to-the ENE shear thrusting, map-scale recumbent folding and sinistral shearing (D_1) and (2) N- to NE-vergent fold-and-thrust tectonics contemporaneous with wildflysch sedimentation (D_2). The two are kinematically compatible within a framework of D_{1-2} partitioned sinistral transpression along a ENE (i.e., Cévennes) structural trend (Fig. 1b). The consistent regional ENE trend of the stretching lineations is not perturbed by F_2 folding (Figs. 2 and 5b) as F_2 folds, intersection lineations and stretching lineations are statistically undistinguishable (Fig. 3c) and parallel to microfold and crenulation axes (Lee, 1988). Coincidence of the macroscopic recumbent (sheath) fold axes and the stretching lineations is consistent with fold amplification / reorientation by simple shearing (Berthé and Brun, 1980; Cobbold and Quinquis, 1980) further enhanced by shear-perpendicular (D_2) shortening. The remaining spread in fold directions around the ENE trend would be indicative of various degrees of reorientation of F_1 folds towards the shear direction (e.g., Franke et al. 2011). S_{1-2} is axial-planar to the macroscopic recumbent folds but is also folded around the Le Lau antiform (Fig. 5a) and at the same time axial-planar to the Laurenque sheath synform (Figs. 3a, 4a and 5a) and to the F_2 folds further to the East in the Monts de Faugères. The S_{1-2} triple point at the eastern termination of the Laurenque synform further argues for interference between eastward amplification of the fold and NNW-directed (D_2) shortening. These considerations are indicative of an overlap in time between eastward shearing (D_1) and F2-related shortening (D_2) in a common D_{1-2} kinematic frame.

Series overturning has been achieved essentially eastwardly (Fig. 9), in agreement with eastward shear thrusting. The overall structure of the Pardailhan unit is in fact that of an ENE-facing sheath anticline underlined by the Cambrian massive series (see cross-sections of Echtler,

362 1990). Superimposition of ENE F_2 folding on regional-scale F_1 ENE-verging recumbent
363 anticlines and synclines produced east-facing sheath anticlines (the Pardailhan anticline, the
364 Roquebrun synformal anticline and, to a lesser extend, the fold NW of Cabrières) and W-facing
365 sheath synclines (Le Lau antiform), respectively (Fig. 3b). The present example therefore shows
366 that transpression with a major component of longitudinal shearing (i.e., wrench dominated) can
367 produce regional-scale, wrench-parallel recumbent sheath folds.

368 Early syn-flysch ($D_{1)}$ fold-and-thrusting is illustrated by the progressive unconformity at
369 the northeastwardly overturned backlimb of the Orb syncline (Fig. 4b). This, together with the
370 regional northeastward regional stratigraphic polarity of the wildflysch (Fig. 2), indicates that
371 early NE-verging fold-and-thrusting set the first-order geometry of the wildflysch basin.
372 Younger progressive unconformities in the wildflysch attesting to more pronounced northward
373 progradation (e.g., Laurens area; Figs. 2 and 4c) suggest a later control of northward fold-and-
374 thrusting on flysch sedimentation. This, together with the large-scale F_1/F_2 interference pattern,
375 indicates that ENE-vergent thrusting (D_1) started before northward fold-and-thrust tectonics (D_2).
376 The onset of eastward thrusting is constrained by the first occurrences of calciturbidites along the
377 overturned limb of the Orb syncline (Fig. 4b), testifying to the destabilization of the carbonate
378 platform topping the Mont Peyroux anticline in its early amplification stages. Vachard et al.
379 (2017) reported a mid-Viséan (Livian) age (~340-336 Ma) for those calciturbidites. The late
380 Serpukhovian age of the youngest dated olistoliths in the wildflysch (near Cabrières) indicates
381 that northeastward fold-and-thrusting was still active or had ceased by ~323 Ma (end
382 Serpukhovian; Vachard et al., 2017), because the flysch hosting these olistoliths is involved in
383 the Écailles de Cabrières folds and thrusts. Left-lateral $D_{1\text{-}2}$ transpressional fold-and-thrust
384 tectonics therefore took place after 340 Ma over a ~20 Myr period.

385

386 ***5. 2. Late Right-Lateral Transtensional Tectonics***

387 Tectonic contacts formed by sinistral transpression (D_{1-2}) have been reactivated by dextral
388 transtension (D_3) through a system of normal-oblique faults and décollement(s) along which
389 strain localization took place in the presence of fluids. Dextral transtension took place along
390 shear bands and shear zones distributed in the northern deformation zone that earlier recorded
391 pervasive sinistral shearing. In the Margal-Mons area (Fig. 2), the outer dome and Schistes X
392 have Ar-Ar muscovite and biotite ages of 308 +/-3 Ma (Maluski et al., 1991) and K-Ar
393 muscovite ages of 297-292 Ma (Franke et al., 2011), whereas the parautochtonous unit has
394 muscovite and biotite Ar-Ar ages of 297 +/-3 Ma (Maluski et al., 1991). These ages are
395 consistent with partial melting and granite emplacement contemporaneous with extensional
396 deformation and detachment faulting in the Axial Zone as refined to 317-294 Ma by TIMS, LA-
397 ICPMS, and SIMS U-Th-Pb dating (Franke et al., 2011; Poilvet et al., 2011; Pitra et al., 2012;
398 Roger et al., 2015, 2020; Poujol et al., 2017; Trap et al., 2017). The shift from sinistral
399 transpression to dextral transtension therefore took place between 323 Ma (minimum
400 stratigraphic age of thrusting) and 317 Ma.

401

402 **6. Discussion**

403 ***6. 1. Nappe tectonics in the Montagne Noire***

404 Sinistral transpressive fold-and-thrust tectonics of the Southern Montagne Noire accounts at last
405 for paleogeography. Such kinematics indeed imply a southwestern origin for the “nappes”, as
406 opposed to an elusive source north of the Axial Zone. It is also consistent with the Écailles de
407 Cabrières being exotic in the Montagne Noire and part of a southern province including the

Mouthoumet massif and the Pyrenees (Fig. 1b). The model also provides a mechanism for producing ENE recumbent folds with their axes parallel to the main direction of shearing, which is responsible for the main and only pervasive deformation pattern in the southeastern Montagne Noire. This prompts abandonment of the southward nappe emplacement paradigm and therefore also challenges models interpreting the Axial Zone as hosting a N-dipping crustal-scale thrust and/or being a stack of duplexes or pennic-like fold nappes pilled-up from the north (Graham et al., 1987; Soula et al., 2001; Matte, 2007; Malavieille, 2010; Faure et al., 2014). In the end, our results support the original model of Gèze (1949) in which the northern and southern thrust belts of the Montagne Noire have opposite vergencies towards the Axial Zone.

Lee et al. (1988) came to an interpretation comparable to ours for the deep deformation pattern of the Southeastern Montagne Noire as being possibly related to original eastward "nappe" emplacement. But they also considered the alternate possibility for this deformation to result from a "reorientation" of originally N-S nappe-related lineations. As recalled by Franke et al. (2011), such stretching lineations preexisting the penetrative deformation pattern of Figure 5 do not exist.

Franke et al. (2011) proposed a post-nappe D_2-D_3 deformation model somehow comparable to our $D_{1\text{-}2}$ model in its description. But if their D_3 matches our F_2-related shortening, their D_2 is interpreted as ENE-directed extension. This however contradicts the dextral slip these authors evoke along the northern deformation belt at the time of that extension, for eastward shearing implies sinistral slip there, which is actually the case (Fig. 5c). ENE extension envisioned by Franke et al. (2011) was interpreted to be coeval with HT-LP metamorphism of the Axial Zone and shearing at the dome's margin at 314-306 Ma, prior to ENE (F_2) folding (Doublier et al., 2015). But as shown here, F_2 folds grew during flysch

sedimentation i.e., essentially before 323 Ma. Contrary to extension, sinistral transpression provides for the first time a kinematic scheme for producing recumbent folding by ENE shearing, whose pervasiveness and intensity can account for the amplitude of the overturned limbs. Sinistral transpression therefore represents the main and pervasive tectonic episode in the Southern Montagne Noire.

6. 2. Tectonics and flysch sedimentation

The space-time sedimentology patterns of the flysch and its platform carbonate time-equivalent series have been argued to attest to, or to be consistent with, the southward emplacement of the nappes (Engel et al., 1978, 1981; Vachard et al., 2017). It is our opinion that these patterns are compatible with either a northern or a southern origin. But the newly documented progressive unconformities in the wildflysch are consistent with progradation in the same sense as D_2 fold-and-thrust propagation. This would also be consistent with, for instance, the Monts de Faugères flysch being more distal than the Mont Peyroux – Laurens flysch (e.g., Engel et al., 1981; Vachard et al. 2017; Figs. 2 and 4b). Syn-sedimentary gliding patterns in the wildflysch (Fig. 5c) suggest gliding on the slopes of shallowly WSW-plunging F_2 synclines, consistently with WSW gliding documented in the mass transport complex (Fig. 8c). Poor preservation of northward gliding features may be explained by the fact that the northward slope forming the forelimbs of north-verging anticlines are preferentially affected by north-vergent thrust deformation that overprinted them (e.g., Figs. 7c, 8a and 8c). More generally, the spatial sedimentological pattern of the flysch would have been controlled at the scale of anticline / syncline pairs, with the platform carbonates having tried to maintain on the upper backlimbs and crests of northward-verging F_2 anticlines and more distal flysch in F_2 synclines. Likewise,

variation in the Carboniferous stratigraphy among the Écailles de Cabrières (Engel et al., 1981; Aretz, 2016; Vachard et al., 2017) would be explained by the fact that they originate from folds with contrasted uplift histories.

6. 3. Cévennes fault kinematics

The Montagne Noire represents a portion of the >500 km-long Cévennes fault (Arthaud and Matte, 1975; e.g., Fig. 1), which bounded the Devonian- Carboniferous sedimentary basin to the NW and must have had somehow a SE-side-down throw to allow Devonian and Tournaisian sedimentation (until ~345 Ma) that did not take place in its northwestern hangingwall. That early fault history may tentatively be linked to late Devonian NW-directed shearing affecting the hinterland (Duguet and Faure, 2004) and could have recorded orogen-parallel extension at a time of back-arc basin opening in the Northeastern Massif Central (Faure et al., 2009).

Shortly after 340 Ma and until ca. 323 Ma (stratigraphic dating of deformation), the Cévennes fault underwent sinistral transpression. It was reactivated as a dextral transtensional fault during dome exhumation after 317 Ma. The dextral releasing bend of the Cévennes fault in the Montagne Noire is therefore interpreted to result from the inversion of a preexisting sinistral restraining bend (Fig. 10).

Our investigation of the eastern part of the northern thrust belt (Monts de Lacaune; Fig. 1b) revealed a system of thrust duplexes affected by pervasive shallowly dipping shears with systematic top-to-the-SSE (N160°E) sense of slip. In the easternmost unit, the Mendic granitic pluton represents a sheet in that shear system affected by a strong fabric with the same shear sense. Ar-Ar muscovite dating in the pluton (Costa, 1990) indicates that southward thrusting was active at 333 +/- 4 Ma. But more generally, Ar-Ar and K-Ar dating constrains activity of the

477 northern thrust belt from 342 Ma until after 328 Ma (Costa, 1990; Doublier et al., 2006). SSE-
478 directed thrust shearing implies sinistral transpression along the NE-striking thrusts of the
479 northern thrust belt and along the Cévennes fault, even considering the 20° of counter-clockwise
480 rotation undergone by the thrust system during transtension (Cogné et al., 1990; Fig. 9).
481 Kinematics of the southern and northern thrust belts were therefore linked during sinistral
482 transpression along the restraining bend of the Cévennes fault at ~340-323 Ma.
483 The pervasiveness of sinistral shearing in the Caroux sub-dome of the Axial Zone
484 (Beaud, 1985; Schranzhofer, 1999) and its southern envelope (Lee, 1988; present study)
485 indicates that part of the Axial Zone was involved in the sinistral Cévennes shear zone (Fig. 10).
486 The superimposition of dextral shearing on sinistral transpression required by the present
487 reappraisal of thrust tectonics should open new perspectives on the disputed internal deformation
488 of the gneiss dome (Ellenberger, 1967; Beaud, 1985; Matte et al., 1998; Schranzhofer, 1999; Rey
489 et al., 2011, 2012, 2017; Van Den Driessche and Pitra, 2012; Rabin et al., 2015; Roger et al.,
490 2020). In any case, the present work provides a kinematic scheme for crustal thickening within
491 the bend during early sinistral transpression. Eclogite boudins in the Caroux gneisses have
492 provided two sets of geochronological ages (360 and 315 Ma), both obtained independently by
493 two research groups (Faure et al., 2014; Whitney et al., 2015). The oldest age retained by Faure
494 et al. (2014) as that of eclogite metamorphism is not reconcilable with the sedimentary record
495 characterized by regionally distributed and homogeneous chert / carbonate sedimentation at the
496 time (Aretz, 2016) and the fact that thrusting took place after 340 Ma (maximum stratigraphic
497 age of thrusting). Alternatively, if valid (but still unlikely), the 360-Ma eclogite metamorphism
498 hypothesis would imply complete decoupling between the thickening gneissic core (Caroux) of
499 the shear zone and the Paleozoic series. The 315 Ma age of HP metamorphism favored by

500 Whitney et al. (2015) would imply that the Caroux gneisses were at ~30 km depth at the onset of
501 transtensional exhumation of the Axial Zone (317 Ma). But burial, if any, to HP conditions by
502 sinistral transpression would still be older (>320 Ma, the minimum age of thrusting).
503
504 ***6. 4. Orogen-scale transcurrent faulting and orocline bending***
505 Variscan convergent deformation in the southern Massif Central took place from ~342 to 323 Ma
506 across a >80 km wide sinistral transpressive fold-and-thrust belt centered on the Cévennes fault,
507 forming a restraining bend in the Montagne Noire (Fig. 10a). Sinistral transpression responded to
508 far-field (plate boundary driven) convergence. The shift to dextral transtension along the
509 Cévennes fault after 317 Ma (Fig. 10b) responded to the amplification of the Iberain-Armorican
510 syntax and final closure of the Cantabrian orocline in its core between 305 and 295 Ma (timing
511 in Weil et al., 2010).
512 Early sinistral kinematics of the Cévennes fault (and, probably, the East Variscan shear
513 zone) between 340 and 323 Ma implies partitioning of convergence in the southern foreland
514 between thrusts and NNE striking sinistral faults (Fig. 11). Such a partitioning requires
515 hinterland-ward (retro) fold-and-thrust tectonics to have taken place as attested to in the Southern
516 Montagne Noire. Besides, field reconnaissance in the Mouthoumet Massif (Fig. 1b) suggests a
517 comparable north-verging transpressive deformation pattern. Various transpressive reliefs must
518 therefore have been produced, at least in the strike-slip corridor formed by the Cévennes fault
519 and the East Variscan shear zone, feeding the flysch with proximal material. This suggests a
520 multiplicity of coeval wildflysch depocenters rather than a foreland-ward succession of younger
521 basins formed by southward propagating pro-thrusts (see Martínez et al., 2016). Retro-thrusts

522 east of the Cévennes fault may be prefiguring the growth of an orocline flanking the Eastern
523 Massif Central and pointing toward the Bohemian massif (Matte, 2001; e.g., Fig. 1a).
524 Dextral transtension along the Cévennes fault from 317 to 294 Ma accompanied
525 gravitational collapse and northeastward escape of the northern limb of the growing syntax (Fig.
526 11) in which convergent deformation had ceased. The Sillon houiller acted as a transfer fault
527 between (1) orogen-parallel extrusion / extension of the wedge escaping from the syntax hinge
528 and (2) orogen-normal extensional collapse guided by the Cévennes-trend faults (Burg et al.,
529 1994). At that time (and until 290 Ma), just SW of the North Pyrenean fault, SW-vergent
530 thrusting as well as orocline limb-parallel extension and dextral strike-slip were taking place in
531 the Axial Zone of the Pyrenees (Cochelin et al., 2017; Figs. 1b and 11). The North Pyrenean
532 fault is therefore a first-order transform fault in the orogen, decoupling the closing orocline from
533 the northern syntax limb undergoing gravitational collapse.
534
535 ***6. 5. Shear sense reversal and exhumation in orogen-scale transcurrent fault systems***
536 Releasing bends along strike-slip fault systems are propitious to the formation of metamorphic
537 core complexes (Denèle et al., 2017). In the Montagne Noire, early transpressional crustal
538 thickening within the bend would be a prerequisite to extensional exhumation in the dextral
539 releasing bend. The restraining bend was indeed a mountain range that had the gravitational
540 potential to spread in the dextral releasing context, further enhancing lower crust advection in the
541 gneiss dome. This would also explain why the Montagne Noire releasing bend is not a pull-apart
542 sedimentary basin but a gneiss dome, with syn-tectonic sediments flanking the releasing bend
543 instead of filling it (e.g., Fig. 1b).

544 Shear sense reversal along long-lived, orogen-scale strike-slip fault systems should be
545 very common, because such fault systems undergo large-magnitude vertical axis-rotation(s) and
546 bending during collision as a consequence of indentation, escape tectonics or orocline bending
547 (Tapponnier et al., 1986; Martínez Catalán, 2011). It is the case for the Cévennes fault, which
548 was active for 50 Myr (340-290 Ma). The fault first contributed to the partitioning of plate
549 convergence and was later incorporated to the hinterland as a transfer fault bounding escaping
550 orogenic domains (Fig. 11).
551
552 **7. Conclusion**
553 Instead of having glided southward, the Paleozoic nappes of the Montagne Noire were thrust
554 northeastwardly during wrench-dominated sinistral transpression along the Cévennes fault
555 between 340 and 323 Ma. Consequently, convergent tectonics of the southern side of the
556 Variscides may be reconsidered, with a foreland basin being decoupled from the hinterland along
557 orogen-scale transcurrent fault(s) trending at a high angle to the orogenic trend. These faults
558 interacted with hinterland-ward thrust systems East of the Cévennes fault, which must have
559 generated a variety of reliefs and adjoining depocenters. Shift to dextral transtension along the
560 Cévennes fault after 317 Ma accompanied closure of the Iberian-Armorican syntax by
561 accommodating northeastward escape and gravitational collapse of the northern limb of the
562 syntax. These results have implications for orogenic-scale kinematic control on shear sense
563 inversion and lower crust exhumation along long-lived transcurrent fault systems.
564
565 **Acknowledgements**

We thank José R. Martínez Catalán, an anonymous referee and editor Philippe Agard for their constructive remarks. Fieldwork was partially supported by a CNRS-INSU SYSTER grant. We acknowledge Arnaud Dalbin and Mouna Nadrani for their participation in the fieldwork.

References

Aerden, D.G.A.M., 1998. Tectonic evolution of the Montagne Noire and a possible orogenic model for syncollisional exhumation of deep rocks, Variscan belt, France. Tectonics 17, 62-79.

Aerden, D.G.A.M., Malavieille, J., 1999. Origin of a large-scale fold nappe in the Montagne Noire, Variscan belt, France. J. Struct. Geol. 21, 1321-1333.

Alabouvette, B., Arthaud, F., Feist, R., Ellenberger, F., Berger, G., 1982a. Carte géologique de la France à 1/50 000, Saint-Chinian (1014). Bur. Rech. Géol. Min., Orléans

Alabouvette, B., Arthaud, F., Feist, R., Médioni, R., Brousse, R., 1982b. Carte géologique de la France à 1/50 000, Lodève (989). Bur. Rech. Géol. Min., Orléans.

Aretz, M., 2016. The Kulm Facies of the Montagne Noire (Mississippian, southern France). Geol. Belg. 19, 69-80.

Arthaud, F., 1964. Étude structurale de la terminaison occidentale des Monts de Faugères (Montagnes Noire, Hérault). Bull. Serv. Carte Géol. Fr. 277, 133-144.

Arthaud, F., 1969. Un exemple de relations entre l'étirement dans B, la dispersion des linéations et la courbure des axes de plis : la virgation des plis couchés hercyniens du versant sud de la Montagne Noire. Rev. Géogr. Phys. Géol. Dyn. XI, 523-532.

Arthaud, F., 1970. Étude tectonique et microtectonique comparée de deux domaines hercyniens : les nappes de la Montagne Noire (France) et l'anticlinorium de l'Iglesiente (Sardaigne). Publ.

589 USTELA, Ser. Géol. Struct. 1, 1-175.
590 Arthaud, F., Burg, J., Matte, P., 1976. L'évolution structurale hercynienne du massif de
591 Mouthoumet (Sud de la France). Bull. Soc. Géol. Fr. 7(XVIII), 967-972.
592 Arthaud, F., Mattauer, M., Proust, F., 1966. La structure et la microtectonique des nappes
593 hercyniennes de la Montagne Noire, Étages tectoniques. La Baconnière, Neuchâtel, pp. 229-
594 241.
595 Arthaud, F., Matte, P., 1975. Les décrochements tardi-hercyniens du Sud-Ouest de l'Europe.
596 Géométrie et essai de reconstitution des conditions de la déformation. Tectonophysics 25,
597 139-171.
598 Ballèvre, M., Bosse, V., Dabard, M.P., Ducassou, C., Fourcade, S., Paquette, J.L., Peucat, J.J.,
599 Pitra, P., 2013. Histoire géologique du Massif Armoricain : Actualité de la recherche. Bull.
600 Soc. Géol. Minéral. Bretagne D, 5-96.
601 Ballèvre, M., Manzotti, P., Dal Piaz, G.V., 2018. Pre-Alpine (Variscan) Inheritance: A Key for
602 the Location of the Future Valaisan Basin (Western Alps). Tectonics 37, 786-817.
603 Beaud, F., 1985. Étude structurale de la Zone Axiale orientale de la Montagne Noire (Sud du
604 Massif Central français). Détermination des mécanismes de déformation. Relation avec les
605 nappes du versant sud. PhD Thesis, Université des Sciences et Techniques du Languedoc,
606 Montpellier, 191p.
607 Bergeron, J., 1904. Sur les nappes de recouvrement du versant méridional de la Montagne Noire.
608 C.R. Acad. Sci. Paris 138, 394-395.
609 Berthé, D., Brun, J.P., 1980. Evolution of folds during progressive shear in the South Armorican
610 shear zone, France. J. Struct. Geol. 2, 127-133.
611 Bogdanoff, S., Donnot, M., Becq-Giraudon, J.F., Boulanger, A.H., Demange, M., Ellenberger,

612 F., Freytet, P., Ildefonse, J.P., Latouche, L., Pinna, P., Prunac, M., Rolet, J., Santarelli, N.,
613 Quesnardel, J.M., 1982. Carte géologique de la France à 1/50 000, Bédarieux (988). Bur.
614 Rech. Géol. Min., Orléans.
615 Burg, J., Matte, P., 1978. A cross section through the French Massif Central and the scope of its
616 Variscan evolution. Z. dt. geol. Ges. 129, 429-460.
617 Burg, J., Van Den Driessche, J., Brun, J., 1994. Syn- to post-thickening extension in the Variscan
618 belt of Western Europe: Modes and structural consequences. Géol. Fr. 3, 33-51.
619 Cassard, D., Feybesse, J.L., Lescuyer, J.L., 1993. Variscan crustal thickening, extension and late
620 overstacking during the Namurian-Westphalian in the Western Montagne Noire.
621 Tectonophysics 222, 33-53.
622 Chantraine, J., Autran, A., Cavelier, C., Alabouvette, B., Barféty, J.C., Cecca, F., Clozier, L.,
623 Debrand-Passard, S., Dubreuilh, J., Feybesse, J.L., Guennoc, P., Ledru, P., Rossi, P., Ternet,
624 Y., 1996. Carte géologique de la France à 1/1 000 000. Bur. Rech. Géol. Min., Orléans.
625 Charles, N., Faure, M., Chen, Y., 2009. The Montagne Noire migmatitic dome emplacement
626 (French Massif Central): new insights from petrofabric and AMS studies. J. Struct. Geol. 31,
627 1423-1440.
628 Cobbold, P.R., Quinquis, H., 1980. Development of sheath folds in shear regime. J. Struct. Geol.
629 2, 119-126.
630 Cochelin, B., Chardon, D., Denèle, Y., Gumiaux, C., Le Bayon, B., 2017. Vertical strain
631 partitioning in hot Variscan crust: Syn-convergence escape of the Pyrenees in the Iberian-
632 Armorican syntax. Bull. Soc. Geol. Fr. 188, 25.
633 Cogné, J.P., Brun, J.P., Van Den Driessche, J., 1990. Paleomagnetic evidence for rotation during
634 Stephano-Permian extension in the Southern Massif Central (France). Earth Planet. Sci. Lett.

101, 272-280.

Collomb, P., Ellenberger, F., 1965. Age relatif et signification de la linéation régionale dans la Montagne Noire (Massif du Caroux et ses enveloppes, Hérault). C.R. Acad. Sci. Paris Sér. II 261, 195-198.

Costa, S., 1990. De la collision continentale à l'extension tardi-orogénique : 100 millions d'années d'histoire varisque dans le Massif Central français. Une étude chronologique par la méthode 40Ar/39Ar. PhD Thesis, Université des Sciences et Techniques du Languedoc, Montpellier, 441p.

Demange, M., 1998. Contribution au problème de la formation des dômes de la Zone axiale de la Montagne Noire : Analyse géométrique des plissements superposés dans les séries métasédimentaires de l'enveloppe. Implications pour tout modèle géodynamique. Géol. Fr. 4, 3-56.

Denèle, Y., Roques, D., Ganne, J., Chardon, D., Rousse, S., Barbey, P., 2017. Strike-slip metamorphic core complexes: Gneiss domes emplaced in releasing bends. Geology 45, 903-906.

Doublier, M.P., Potel, S., Wemmer, K., 2006. Age and grade of metamorphism in the eastern Monts de Lacaune - Implications for the collisional accretion in Variscan externides (French Massif Central). Geodin. Acta 19, 391-407.

Doublier, M.P., Potel, S., Wemmer, K., 2015. The tectono-metamorphic evolution of the very low-grade hangingwall constrains two-stage gneiss dome formation in the Montagne Noire (Southern France). J. Metam. Geol. 33, 71-89.

Duguet, M., Faure, M., 2004. Successive shearing tectonics during the Hercynian collisional evolution of the southwestern French Massif Central. Bull. Soc. Géol. Fr. 175, 49-59.

Echtler, H., 1990. Geometry and kinematics of recumbent folding and low-angle detachment in

658 the Pardailhan nappe (Montagne Noire, Southern French Massif Central). Tectonophysics
659 177, 109-123.
660 Echtler, H., Malavieille, J., 1990. Extensional tectonics, basement uplift and Stéphano-Permian
661 collapse basin in a late Variscan metamorphic core complex (Montagne Noire, Southern
662 Massif Central). Tectonophysics 177, 125-138.
663 Ellenberger, F., 1967. Replis de micaschistes et tectonique d'infrastructure au sein du massif
664 gneissique du Caroux (zone axiale de la Montagne Noire). C.R. Som. Soc. Géol. Fr. 6, 227-
665 228.
666 Ellenberger, F., 1980. Le Paléozoïque au Sud du Massif Central : Montagne Noire et Massif de
667 Mouthoumet, in: Durand-Delga, M. (Ed.), La chaîne des Pyrénées et son avant-pays
668 aquitanien-languedocien. 26ème Congrès Géologique International, Paris, 1980. Bull. C.
669 Rech. Expl. Prod. Elf-Aquitaine Mém., pp. 20-27.
670 Engel, W., 1984. Migration of folding and flysch sedimentation on the southern flank of the
671 Variscan belt (Montagne Noire, Mouthoumet massif, Pyrenees). Z. dt. geol. Ges. 135, 279-
672 292.
673 Engel, W., Feist, R., Franke, W., 1978. Synorogenic gravitational transport in the Carboniferous
674 of the Montagne Noire (S-France). Z. dt. geol. Ges. 129, 461-472.
675 Engel, W., Feist, R., Franke, W., 1981. Le Carbonifère anté-stéphanien de la Montagne Noire :
676 rapports entre mise en place des nappes et sédimentation. Bull. BRGM 4, 341-389.
677 Faure, M., Cocherie, A., Gache, J., Esnault, C., Guerrot, C., Rossi, P., Wei, L., Li, Q.L., 2014.
678 Middle Carboniferous intracontinental subduction in the Outer Zone of the Variscan Belt
679 (Montagne Noire Axial Zone, French Massif Central): multimethod geochronological
680 approach of polyphase metamorphism. Geol. Soc. Spec. Publ. 405, 289-311.

681 Faure, M., Cottereau, N., 1988. Données cinématiques sur la mise en place du dôme
682 migmatitique carbonifère moyen de la zone axiale de la Montagne Noire (Massif Central,
683 France). C.R. Acad. Sci. Paris 307, 1787-1794.
684 Faure, M., Lardeaux, J.M., Ledru, P., 2009. A review of the pre-Permian geology of the Variscan
685 French Massif Central. C. R. Géosci. 341, 202-213.
686 Feist, R., Berger, G., Freytet, P., 1981. Carte géologique de la France à 1/50 000, Pézenas
687 (1015). Bur. Rech. Géol. Min., Orléans.
688 Franke, W., Doublier, M.P., Klama, K., Potel, S., Wemmer, K., 2011. Hot metamorphic core
689 complex in a cold foreland. Int. J. Earth Sci. 100, 753-785.
690 Franke, W., Engel, W., 1986. Synorogenic sedimentation in the Variscan belt of Europe. Bull.
691 Soc. Géol. Fr. 8(II), 25-33.
692 Gèze, B., 1949. Étude géologique de la Montagne Noire et des Cévennes méridionales. Mém.
693 Soc. Géol. Fr. 62, 1-215.
694 Gèze, B., de Sitter, L., Trümpy, R., 1952. Sur le sens de déversement des nappes de la Montagne
695 Noire. Bull. Soc. Géol. Fr. 6(II), 491-535.
696 Graham, R., Hossack, J., Déramond, J., Soula, J.C., 1987. Géométrie des surfaces de
697 chevauchement. Bull. Soc. Géol. Fr. 8(III), 169-181.
698 Harris, L.B., Burg, J.P., Sauniac, S., 1983. Strain distribution within the Pardailhan nappe
699 (Montagne Noire, France) and structure of its basal thrust zone. Implications for events
700 associated with nappe emplacement. J. Struct. Geol. 5, 431-440.
701 Lee, B.J., 1988. Analyse structurale du versant sud de la Montagne Noire (Hérault - France).
702 Aspects cinématiques de la mise en place des nappes. PhD Thesis, Université d'Orléans,
703 Orléans, 213p.

Lee, B.J., Faure, M., Cluzel, D., Cadet, J.P., 1988. Mise en évidence d'un cisaillement ductile d'ouest en est dans les nappes du versant sud de la Montagne Noire (Sud du Massif Central). C.R. Acad. Sci. Paris Sér. II 306, 455-462.

Malavieille, J., 1993. Late orogenic extension in mountain belts - Insights from the Basin-and-Range and the Late Paleozoic Variscan belt. Tectonics 12, 1115-1130.

Malavieille, J., 2010. Impact of erosion, sedimentation, and structural heritage on the structure and kinematics of orogenic wedges: analog models and case studies. GSA Today 20, 4-10.

Maluski, H., Costa, S., Echtler, H., 1991. Late Variscan tectonic evolution by thinning of earlier thickened crust - an 40Ar-39Ar study of the Montagne Noire, Southern Massif Central, France. Lithos 26, 287-304.

Martínez-Catalán, J.R., 2011. Are the oroclines of the Variscan belt related to late Variscan strike-slip tectonics? Terra Nova 23, 241-247.

Martínez-Catalán, J.R., Pascual, F.J.R., Montes, A.D., Fernandez, R.D., Barreiro, J.G., Dias da Silva, I., González Clavijo, E., Ayarza, P., Alcock, J.E., 2014. The late Variscan HT/LP metamorphic event in NW and Central Iberia: relationships to crustal thickening, extension, orocline development and crustal evolution. Geol. Soc. Spec. Publ. 405, 225-247.

Martínez, F.J., Dietsch, C., Aleinikoff, J., Cires, J., Arboleya, M.L., Reche, J., Gómez-Gras, D., 2016. Provenance, age, and tectonic evolution of Variscan flysch, southeastern France and northeastern Spain, based on zircon geochronology. Geol. Soc. Am. Bull. 128, 842-859.

Mattauer, M., Laurent, P., Matte, P., 1996. Plissement hercynien synschisteux post-nappe et étirement subhorizontal dans le versant sud de la Montagne Noire (Sud du Massif Central, France). C.R. Acad. Sci. Paris Sér. II 322, 309-315.

Mattauer, M., Proust, F., 1963. Sur le déversement vers le Sud et le style tectonique en têtes

727 plongeantes des structures hercyniennes du versant sud de la Montagne Noire. C.R. Acad. Sci.
728 Paris Sér. II 257, 3967-3970.
729 Matte, P., 1983. Two geotraverses across the Ibero-Armorican Variscan arc of Western Europe,
730 in: Rast, N., Delany, F.M. (Eds.), Profiles of orogenic belts. AGU Geodynamic series, pp. 53-
731 81.
732 Matte, P., 2001. The Variscan collage and orogeny (480-290 Ma) and the tectonic definition of the
733 Armorica microplate: a review. Terra Nova 13, 122-128.
734 Matte, P., 2007. Variscan thrust nappes, detachments, and strike-slip faults in the French Massif
735 Central: Interpretation of the lineations, in: Hatcher, R.D., Carlson, M.P., McBride, J.H.,
736 Martínez-Catalán, J.R. (Eds.), 4-D Framework of Continental Crust. Geol. Soc. Am. Mem.
737 200, pp. 391-402.
738 Matte, P., Lancelot, J., Mattauer, M., 1998. La zone axiale hercynienne de la Montagne Noire n'est pas
739 un "metamorphic core complex" extensif mais un anticlinal post-nappe à cœur anatectique. Geodin.
740 Acta 11, 13-22.
741 Maurel, M., 1966. Études sur le Dévonien et le Carbonifère inférieur du versant méridional de la
742 Montagne Noire. PhD Thesis, Université de Montpellier, Montpellier, 196p.
743 Nicolas, A., Bouchez, J.L., Blaise, J., Poirier, J.P., 1977. Geological aspects of deformation in
744 continental shear zones. Tectonophysics 42, 55-73.
745 Pinna, P., Prunac, M., 1976. Sur la distinction d'unités tangentielles nouvelles dans les Monts de
746 Faugères, versant sud de la Montagne Noire (feuille à 1/50 000, Bédarieux). Bull. BRGM 6,
747 239-246.
748 Pitra, P., Poujol, M., Van Den Driessche, J., Poilvet, J.C., Paquette, J.L., 2012. Early Permian
749 extensional shearing of an Ordovician granite: The Saint-Eutrope "C/S-like" orthogneiss

(Montagne Noire, French Massif Central). C. R. Géosci. 344, 377-384.

Poilvet, J.C., Poujol, M., Pitra, P., Van den Driessche, J., Paquette, J.L., 2011. The Montalet granite, Montagne Noire, France: An Early Permian syn-extensional pluton as evidenced by new U-Th-Pb data on zircon and monazite. C. R. Géosci. 343, 454-461.

Poujol, M., Pitra, P., Van Den Driessche, J., Tartese, R., Ruffet, G., Paquette, J.L., Poilvet, J.C., 2017. Two-stage partial melting during the Variscan extensional tectonics (Montagne Noire, France). Int. J. Earth Sci. 106, 477-500.

Rabin, M., Trap, P., Carry, N., Fréville, K., Cenki-Tok, B., Lobjoie, C., Goncalves, P., Marquer, D., 2015. Strain partitioning along the anatectic front in the Variscan Montagne Noire massif (southern French Massif Central). Tectonics 34, 1709-1735.

Ramsay, J.G., Casey, M., Kligfield, R., 1983. Role of shear in development of the Helvetic fold-thrust belt of Switzerland. Geology 11, 439-442.

Rey, P.F., Mondy, L., Duclaux, G., Teyssier, C., Whitney, D.L., Bocher, M., Prigent, C., 2017. The origin of contractional structures in extensional gneiss domes. Geology 45, 263-266.

Rey, P.F., Teyssier, C., Kruckenberg, S.C., Whitney, D.L., 2011. Viscous collision in channel explains double domes in metamorphic core complexes. Geology 39, 387-390.

Rey, P.F., Teyssier, C., Kruckenberg, S.C., Whitney, D.L., 2012. Viscous collision in channel explains double domes in metamorphic core complexes: Reply. Geology 40, e280.

Rodgers, J.G., 1962. L'emploi pratique de la schistosité dans la tectonique locale, in: Durand-Delga, M. (Ed.), Livre Jubilaire Paul Fallot. Mém. h. sér. Soc. Géol. Fr., pp. 83-96.

Roger, F., Teyssier, C., Whitney, D.L., Respaut, J.P., Paquette, J.L., Rey, P.F., 2020. Age of metamorphism and deformation in the Montagne Noire dome (French Massif Central): Tapping into the memory of fine-grained gneisses using monazite U-Th-Pb geochronology.

773 Tectonophysics 776, 228316.
774 Roger, F., Teyssier, C., Respaut, J.P., Rey, P.F., Jolivet, M., Whitney, D.L., Paquette, J.L.,
775 Brunel, M., 2015. Timing of formation and exhumation of the Montagne Noire double dome,
776 French Massif Central. Tectonophysics 640, 53-69.
777 Schranzhofer, C., 1999. La zone de cisaillement polyphasée du versant Sud de la Montagne
778 Noire (Massif Central, France) : Un "vecteur" pour l'exhumation des dômes migmatitiques.
779 PhD Thesis, Université Pierre et Marie Curie, Paris, 197p.
780 Soula, J.C., Debat, P., Brusset, S., Bessiere, G., Christophoul, F., Deramond, J., 2001. Thrust-
781 related, diapiric, and extensional doming in a frontal orogenic wedge: example of the
782 Montagne Noire, Southern French Hercynian Belt. J. Struct. Geol. 23, 1677-1699.
783 Tapponnier, P., Peltzer, G., Armijo, R., 1986. On the mechanics of the collision between India
784 and Asia. Geol. Soc. Spec. Publ. 19, 115-157.
785 Trap, P., Roger, F., Cenki-Tok, B., Paquette, J.L., 2017. Timing and duration of partial melting
786 and magmatism in the Variscan Montagne Noire gneiss dome (French Massif Central). Int. J.
787 Earth Sci. 106, 453-476.
788 Vachard, D., Izart, A., Cózar, P., 2017. Mississippian (Middle Tournaisian-Late Serpukhovian)
789 lithostratigraphic and tectonosedimentary units of the southeastern Montagne Noire (Hérault,
790 France). Géol. Fr. 1, 47-88.
791 Van den Driessche, J., Brun, J.P., 1992. Tectonic evolution of the Montagne Noire (French
792 Massif Central) - A model of extensional gneiss dome. Geodin. Acta 5, 85-99.
793 Van Den Driessche, J., Pitra, P., 2012. Viscous collision in channel explains double domes in
794 metamorphic core complexes: Comment. Geology 40, e279.
795 Von Gaertner, H.R., 1937a. Montagne Noire und Massif von Mouthoumet als Teile des

südwesteuropäischen Variszikums. Abh. Ges. Wissensch. Göttingen, Math.-Phys. III, 1-260.

Von Gaertner, H.R., 1937b. Der Bau des Französischen Zentralplateaus. Geol. Runds. XXVIII, 48-69.

Weil, A., Gutierrez-Alonso, G., Conan, J., 2010. New time constraints on lithospheric-scale oroclinal bending of the Ibero-Armorican Arc: a palaeomagnetic study of earliest Permian rocks from Iberia. J. Geol. Soc. 167, 127-143.

Whitney, D.L., Roger, F., Teyssier, C., Rey, P.F., Respaut, J.P., 2015. Syn-collapse eclogite metamorphism and exhumation of deep crust in a migmatite dome: The P-T-t record of the youngest Variscan eclogite (Montagne Noire, French Massif Central). Earth Planet. Sci. Lett. 430, 224-234.

Wiederer, U., Königshof, P., Feist, R., Franke, W., Doublier, M.P., 2002. Low-grade metamorphism in the Montagne Noire (S-France): Conodont Alteration Index (CAI) in Paleozoic carbonates and implications for the exhumation of a hot metamorphic core complex. Schweiz. Mineral. Petrogr. Mit. 82, 393-407.

Figure Captions

Figure 1. (a) Structural terrane map of the Variscides at the end of the Permian (compiled from Ballèvre et al., 2013, 2018, Burg et al., 1994 and the present work). Iberia, Corsica and Sardinia are shown in their original position relative to continental Europe. (b) Paleozoic geology of the Southern French Massif Central and Eastern Pyrenees (modified after Chantraine et al., 1996 and Faure et al., 2009). Post-Permian cover is shown in white in (a) and (b). Nappe terminology in the Montagne Noire is that of Arthaud (1970).

819

820 **Figure 2.** Geology of the southeastern Montagne Noire based on the present study, adapted from
821 Feist et al. (1981), Engel et al. (1981), Alabouvette et al. (1982a, 1982b) and Bogdanoff et al.
822 (1982). Bedding trajectories in the wildflysch are based mostly on our measurements and those
823 of Engel et al. (1981) (see Fig. S1, supplementary material). The pic de Vissou unit is an
824 overturned slab that has stratigraphic affinities with the Mont Peyroux overturned limb (Engel et
825 al., 1981) and may be considered as one of the Écailles de Cabrières (see Fig. 4f). The inset
826 shows the main area/units mentioned in the text and the interpretative contacts of the Mont
827 Peyroux and Faugères nappes of Arthaud (1970).

828

829 **Figure 3.** (a) Map showing the axial fold traces in the southeastern flank of the Montagne Noire.
830 See Figure 2 for geological caption and locality names. (b) Interpretative three-dimensional fold
831 pattern and axial planes between the western Monts de Faugères and the Mont Peyroux. (c)
832 Synthesis of structural measurements collected east of the Pardailhan unit (equal area, lower
833 hemisphere stereonets).

834

835 **Figure 4.** Simplified cross-sections through the southeastern Montagne Noire. (a) Overall
836 geometry of the F1 Orb syncline in a section perpendicular to the dominant shearing direction.
837 (b) Overturned limb of the F1 Orb syncline (lower part of the section shows an idealized
838 configuration for the F1 Orb syncline without considering F2 folding). (c) Wildflysch basin and
839 Monts de Faugères. (d)-(e) Écailles de Cabrières and Monts de Faugères. (f) Écailles de
840 Cabrières and pic de Vissou unit. The cross-sections are labeled on Figure 2 with red capital
841 letters.

842

843 **Figure 5.** Fabrics and kinematic map patterns of the southeastern Montagne Noire. (a)
844 Schistosity-cleavage. (b) Stretching lineation. (c) Shear criteria and interpretative shear zones.
845 Our kinematic data in (c) are complemented by those of Lee (1988), mostly west of 3°E, and
846 those of Schranzhofer (1999) in the Mons-Margal area (Fig. 2). The insets show a simplified
847 structural map. See Figure 2 for geological caption and locality names.

848

849 **Figure 6.** Top-to the ENE shear deformation patterns in the Monts de Faugères (a-c) and the
850 Mont Peyroux overturned limb (d). (a) Recumbent rootless folds and shear zones in the flysch
851 (shore of Vailhan Lake; 43.564905°N, 3.303711°E). Fold axes are mostly parallel to the
852 stretching lineation. (b) Recumbent sheath fold parallel to the ENE-trending stretching lineation
853 in chert-carbonate associations (East of Faugères; 43.567821°N, 3.223836°E). (c) Devonian
854 marbles West of Cabrières (43.572912°N, 3.325665°E). The ENE-trending lineation (L_{1-2}) is
855 marked by the stretching of carbonate nodules (aspect ratio up to 1:10) and coincides with the
856 intersection between bedding (S_0) and the subhorizontal schistosity (S_{1-2}). (d) Overturned
857 Devonian-Carboniferous contact at the classical Graïs locality (western tip of section:
858 43.534412°N, 2.988400°E). Fold asymmetry and bedding-cleavage relationship in the marbles
859 were used to illustrate southward nappe emplacement (Arthaud, 1964). The structural pattern
860 argues instead for a causal kinematic link between eastward shearing and folding of the marbles
861 that were too competent to allow for complete alignment of the fold axes with the shearing
862 direction, contrary to the other lithologies of the section (see also Lee, 1988). See Figures 2 and 4
863 for locations.

864

Figure 7. Deformation patterns in the flysch of the Écailles de Cabrières unit. (a) Top-to-the NE serial reverse shears (SW of Vailhan; 43.545366°N, 3.294435°E). (b) Olistolith SE of Vailhan (43.551666°N, 3.310578°E). (c) Line drawing of (b). (d) Slip/shear surface measurements shown in (c). Slip surfaces coincide with the layering of a sedimentary slope along which the olistolith and other flysch elements glided. Shear features may be due to syn-sedimentary gliding on a slope or, more likely, tectonic activation of the layering (bed-parallel slip) during N/NE-vergent shearing. Observations in a nearby quarry attest to syn-schistosity - post-sedimentary - top-to-the NE shearing. See Figure 2 for locations.

Figure 8. Field sketches of road / railroad cuts in the flysch of the Écailles de Cabrières unit (a) and the Roquessels mass transport complex (b-c). (a) Olistolith bearing flysch sheared and thrust upon slumped flysch (Castelsec-Fos road; 43.545146°N, 3.241515°E). Northward slump / gliding features are apparently compatible with collapse at the front of the thrust system. (b) Eastern Roquessels mass transport complex (Castelsec-Fos road; southern tip of section: 43.550739°N, 3.234843°E). Low-angle, top-to-the W shearing may be interpreted as prefiguring the Roquessels fault (i.e., Roquessels detachment) or as accompanying westward gliding of the Mass transport complex documented in (c). (c) Westernmost part of the mass transport complex (Malac railroad cut; NW tip of section: 43.548767°N, 3.205925°E). Southeastern part of the section shows a flysch-on-flysch apparent north-vergent thrust comparable to that shown in (a). Rest of the section shows syn-sedimentary top-to-the WSW gliding and normal faulting features. Growth of the mudmound (identified by Vachard et al., 2017) can be shown to have overlapped in time with normal-oblique faulting during top-to-the WSW gliding. Shear measurements are shown by colored stars on the cross-sections. Sections (b) and (c) correspond to East-looking

888 views (North to the left) that have been inverted laterally to follow the convention of all cross
889 sections with North to the right (Fig. 4). See Figures 2 and 4d for locations.
890
891 **Figure 9.** Structural model for the southeastern flank of the Montagne Noire before dextral
892 transtension. The wildflysch is transported as a transpressional piggy-back basin on the Paleo-
893 Roquessels ramp.
894
895 **Figure 10.** Two-stage evolution of the Montagne Noire portion of the Cévennes fault showing a
896 sinistral restraining bend (a) inverted into a dextral releasing bend (b). The structural pattern in
897 (b) takes up and upgrades that of Echtler and Malavieille (1990) by adding, for instance, the
898 Roquessels fault to the southern splays of the Cévennes fault dextral releasing bend. Syn-
899 transtension Stéphano-Permian sediments are omitted.
900
901 **Figure 11.** Sketch model of two late collisional stages of the Southern Variscides showing the
902 Cévennes fault shifting from sinistral to dextral as a consequence of the formation of the Iberian
903 – Armorican syntax. The early stage is reconstructed by restoring the suture zone as a straight
904 line. Fault names: SH – Sillon houiller, CF – Cévennes fault, EVSZ – East Variscan shear zone,
905 NPF – North Pyrenean Fault. Extension directions are mostly after Malavieille (1993), Burg et
906 al. (1994), Martínez-Catalán et al. (2014) and Cochelin et al. (2017).
907

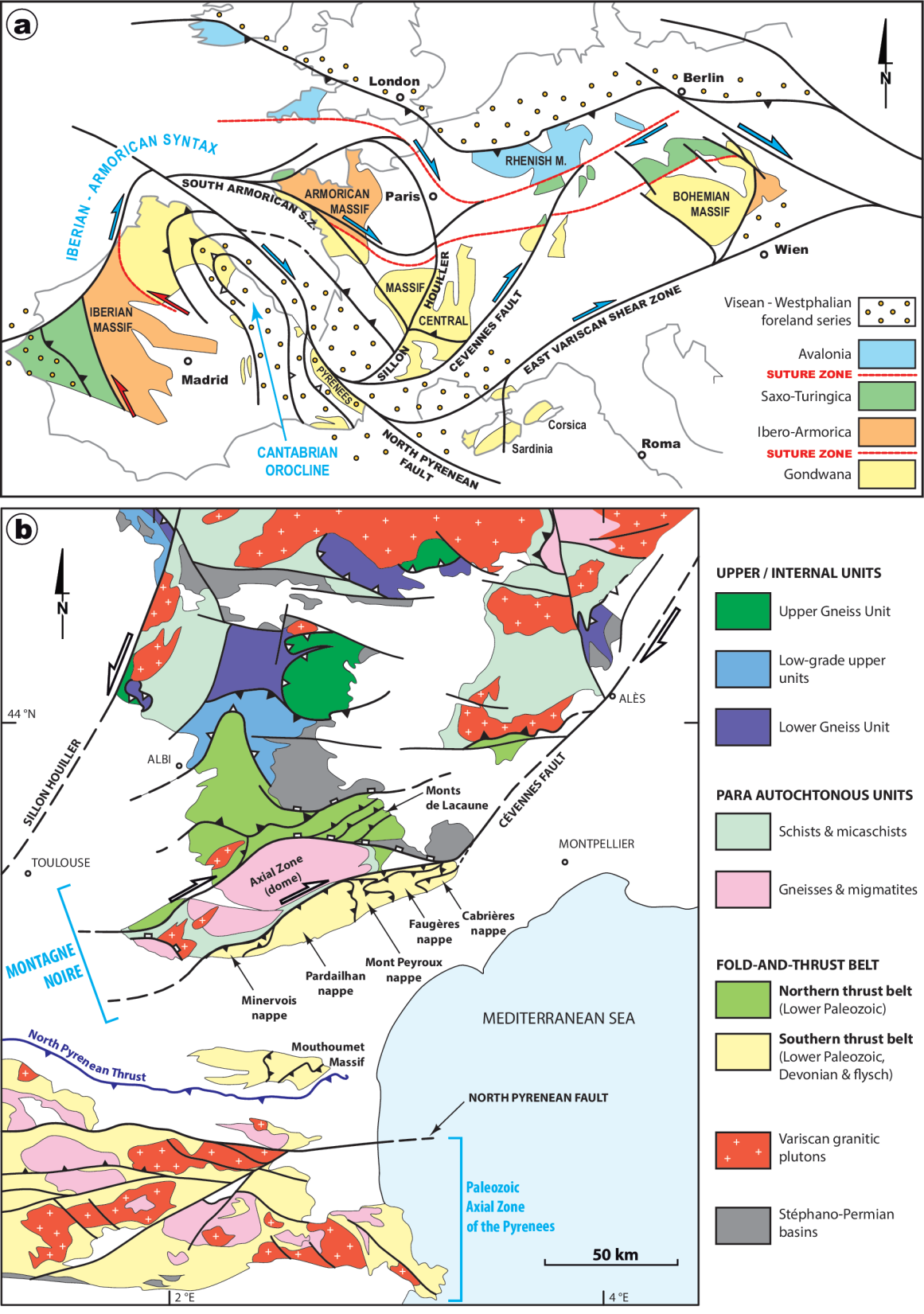

Chardon et al., Fig. 1 (1.5 column)

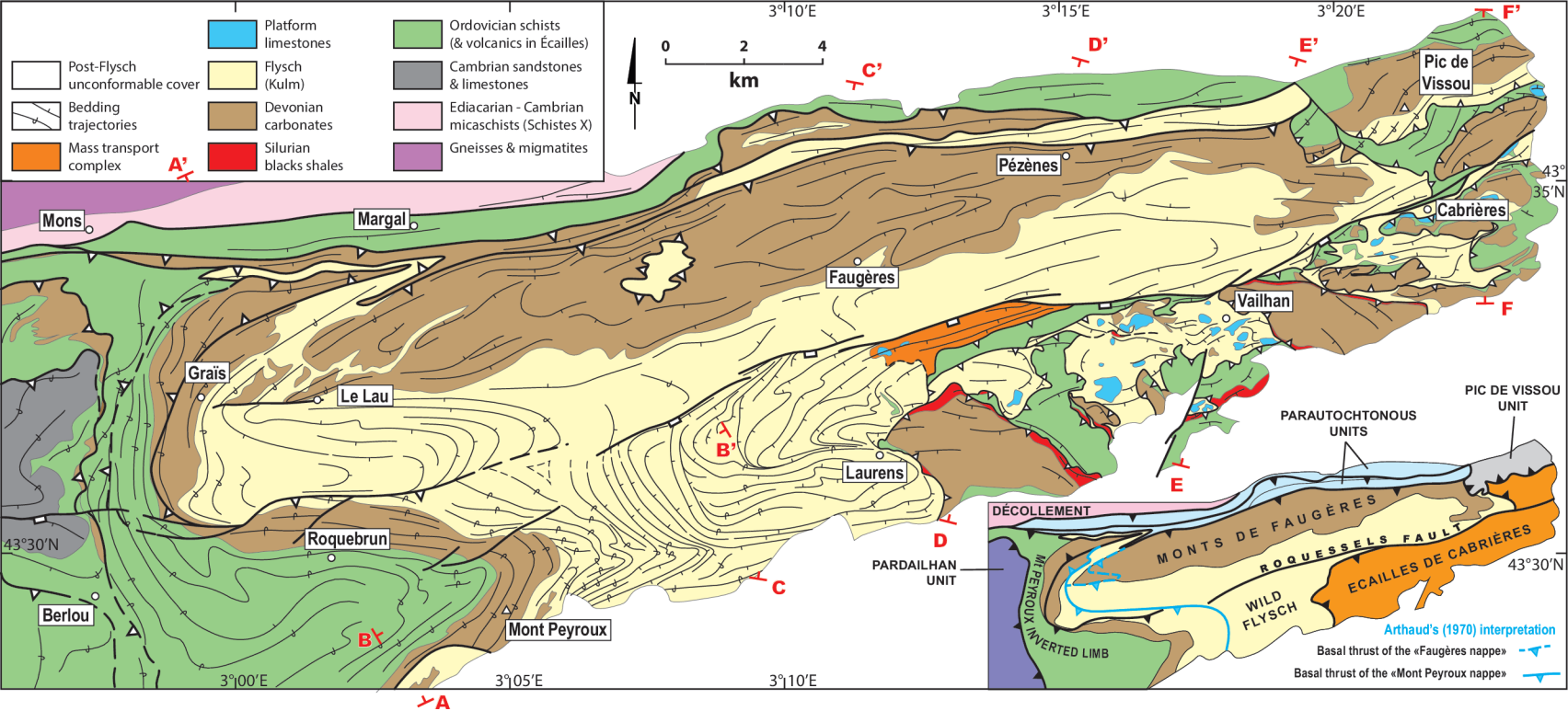

Chardon et al., Fig. 2 Full page, landscape orientation

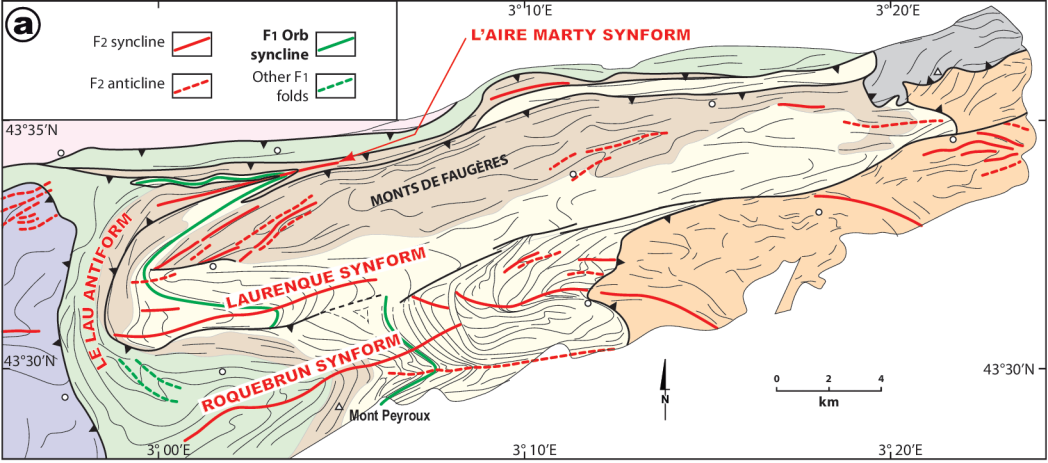

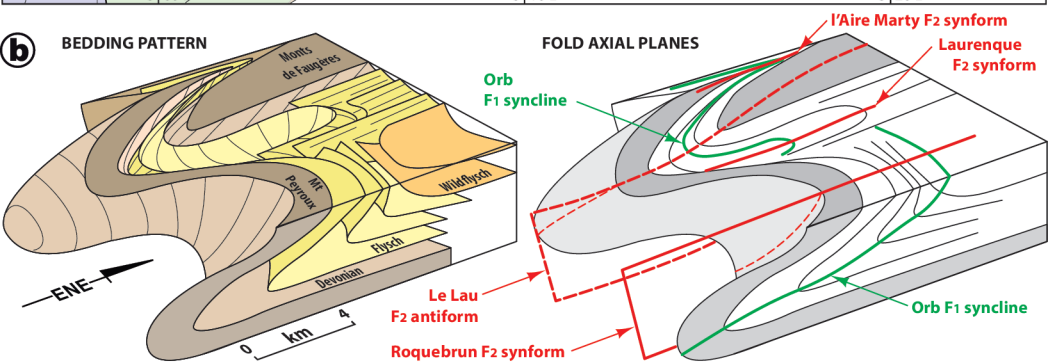

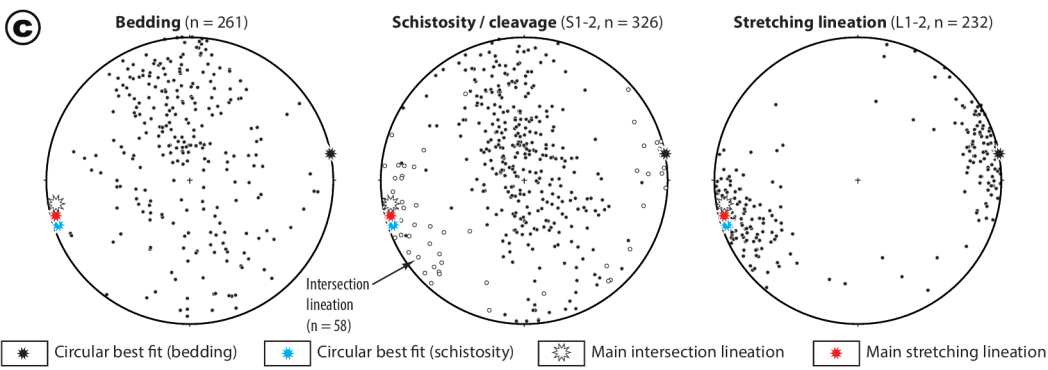

Chardon et al., Fig. 3 (1.5 columns)

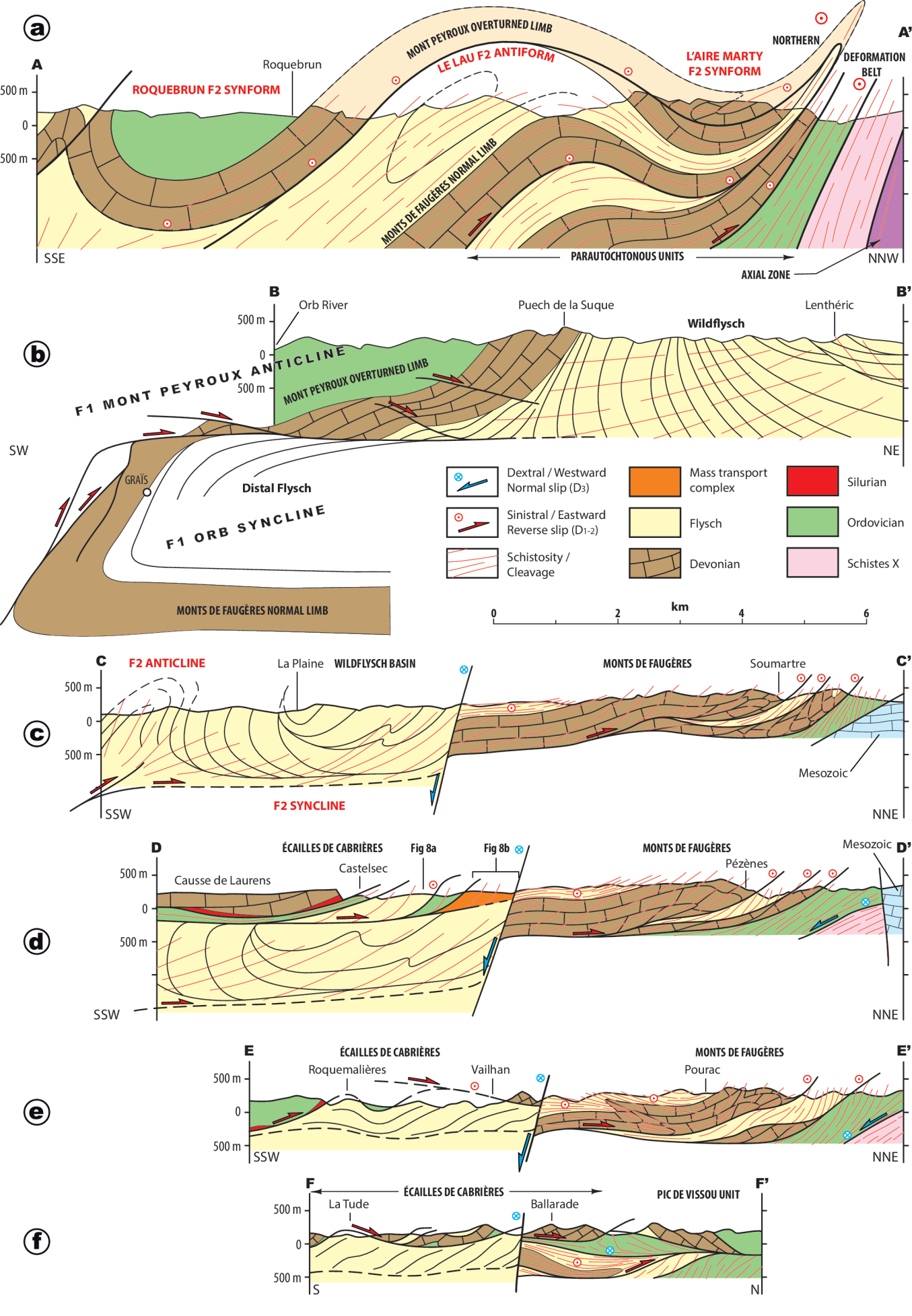

Chardon et al., Figure 4 Full page

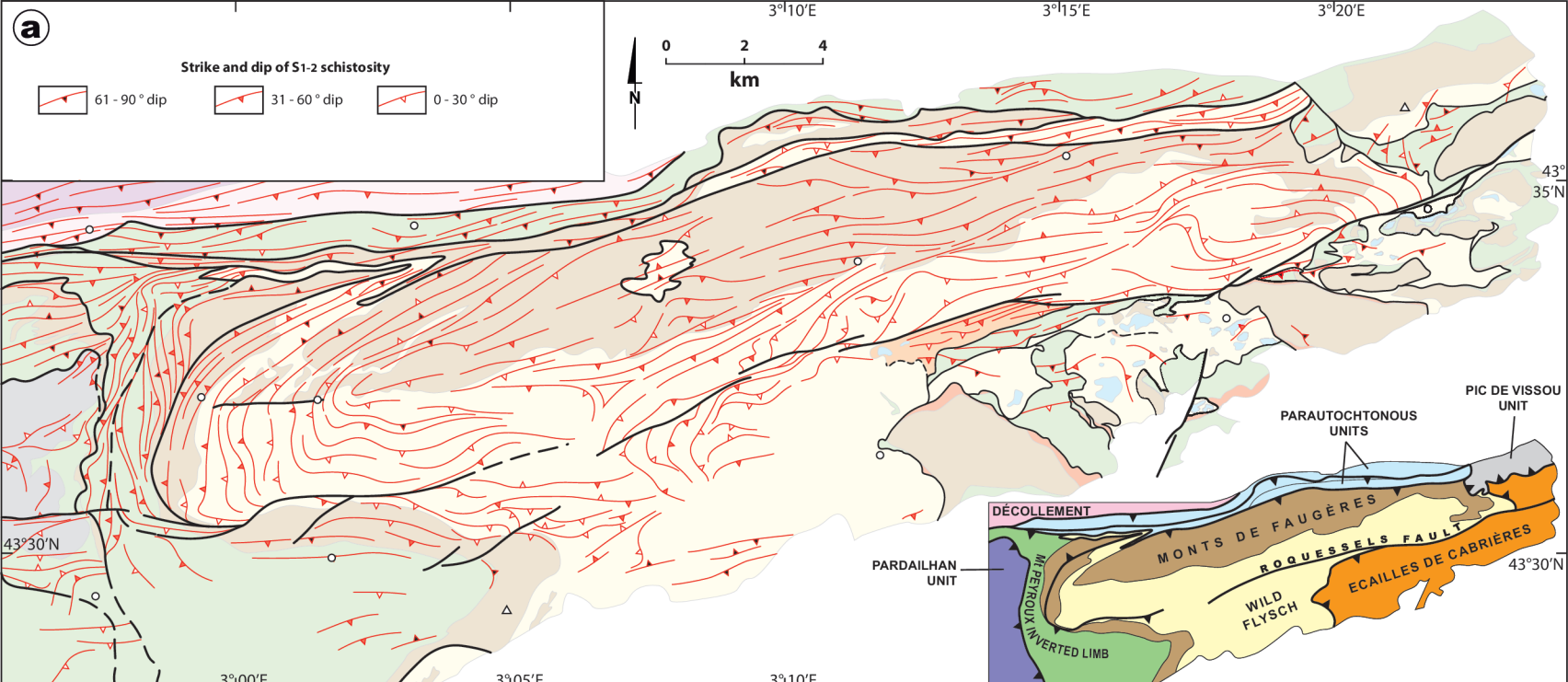

Chardon et al., Fig. 5 Full page, landscape orientation

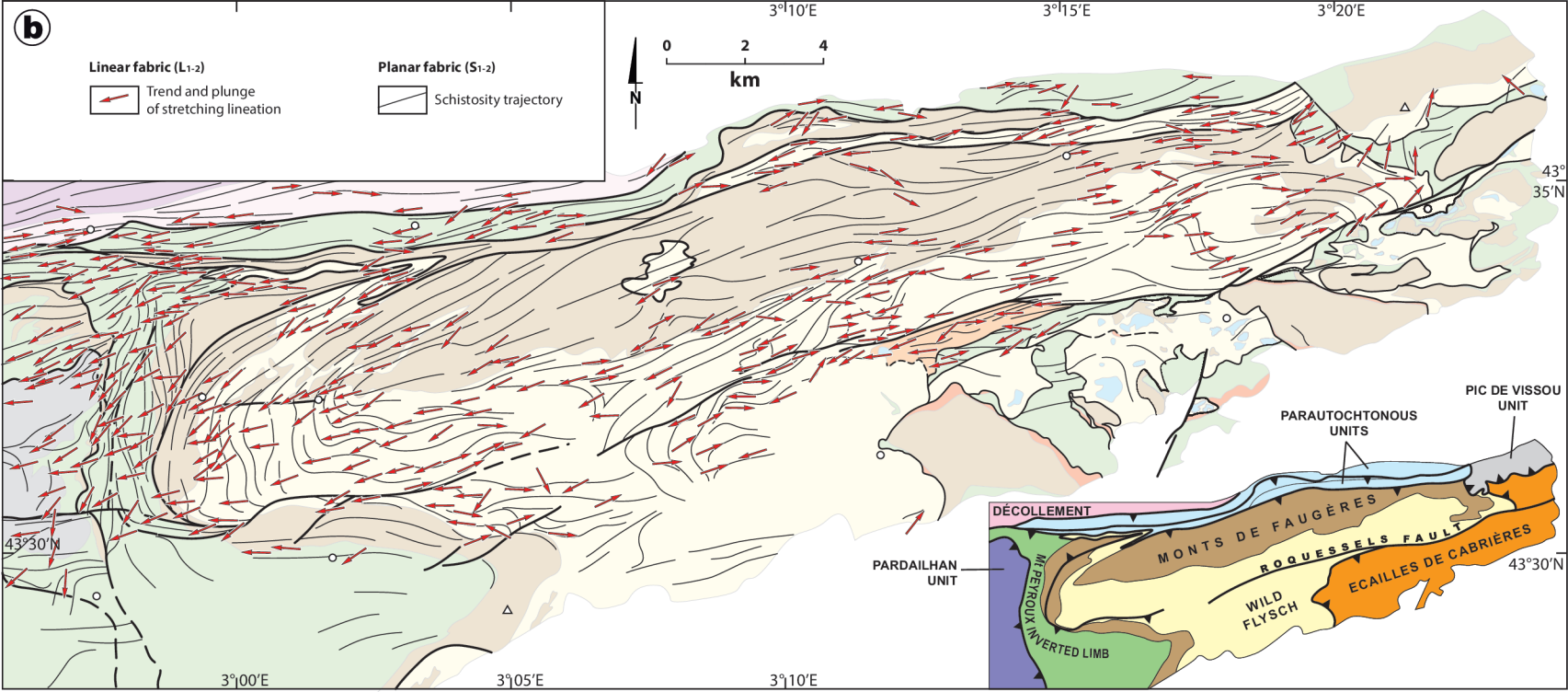

Chardon et al., Fig. 5 (continued) Full page, landscape orientation

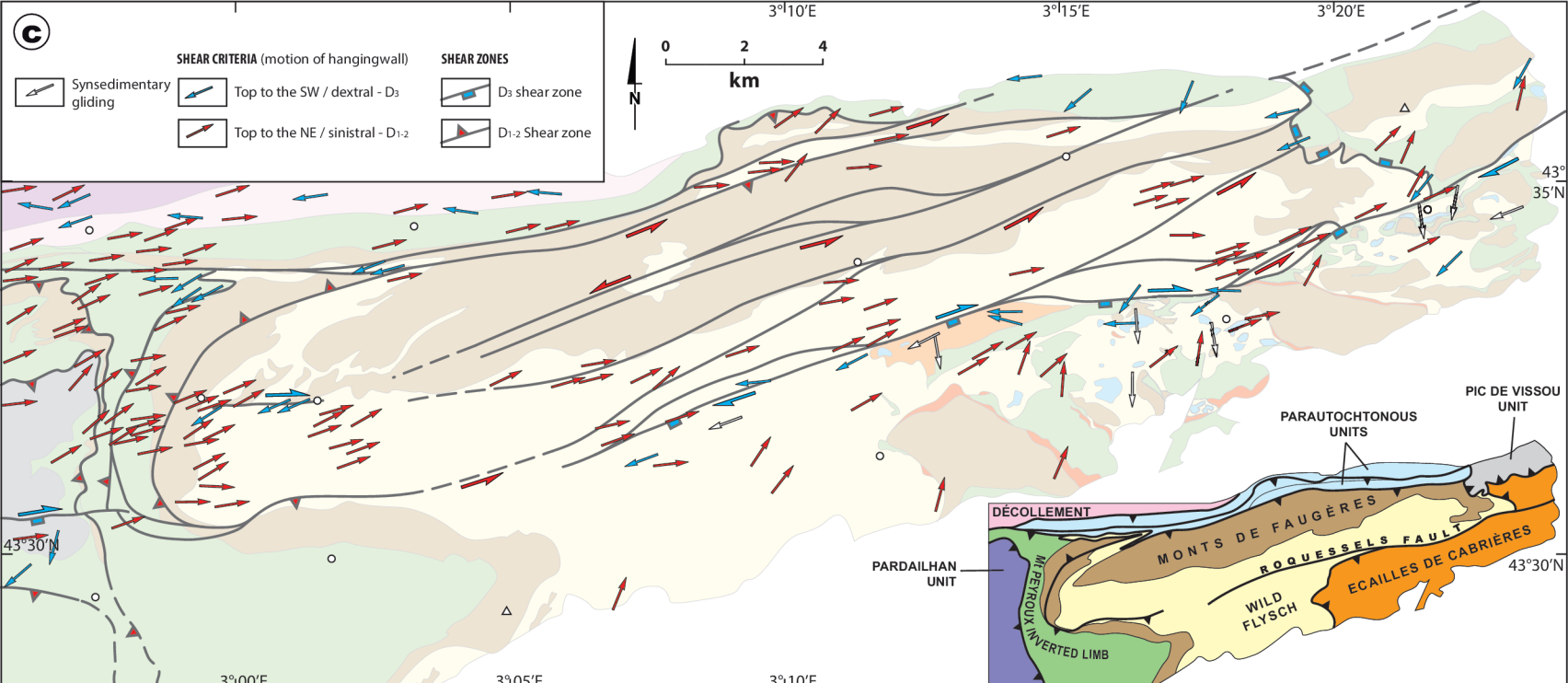

Chardon et al., Fig. 5 (continued) Full page, landscape orientation

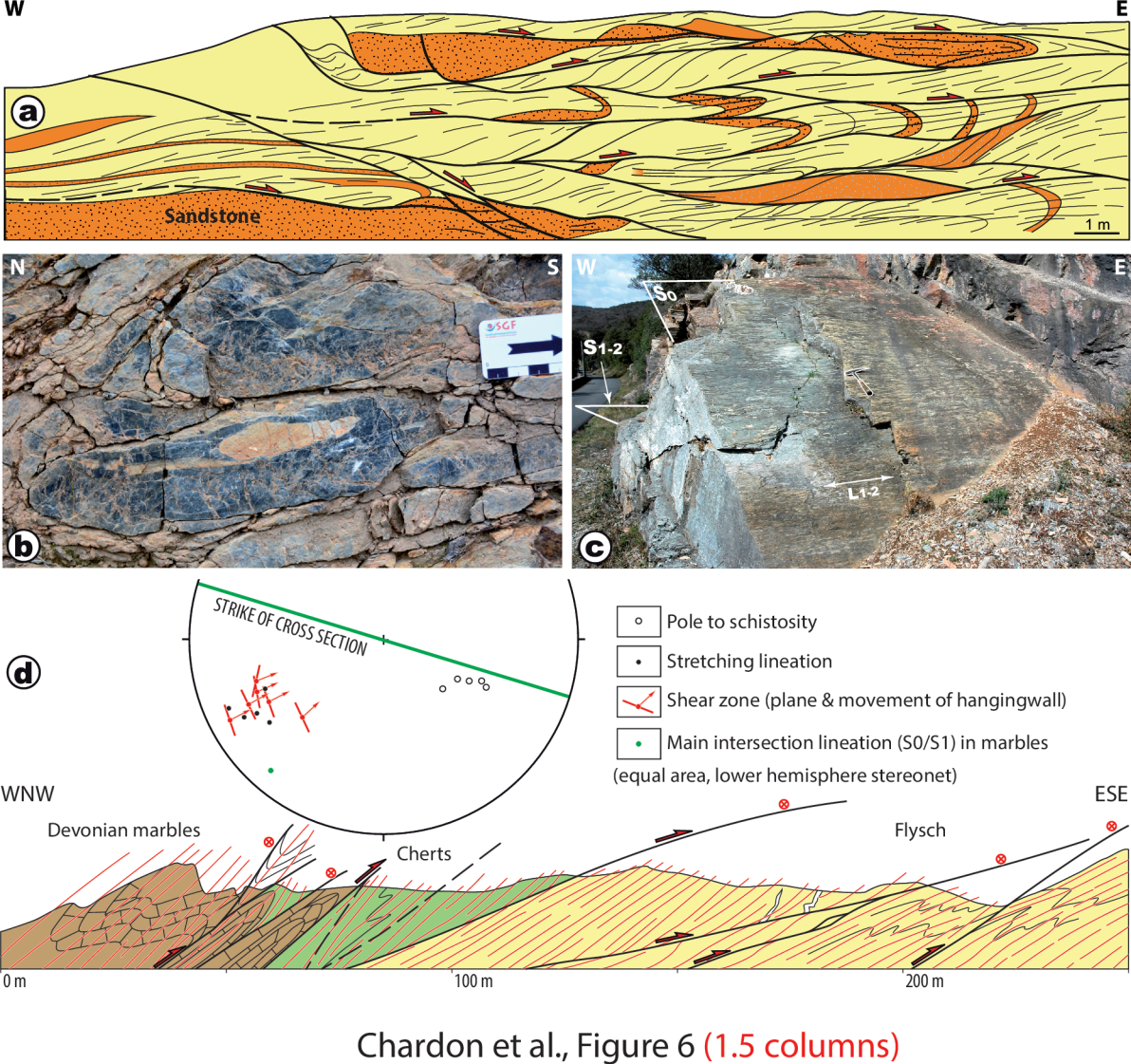

Chardon et al., Figure 6 (1.5 columns)

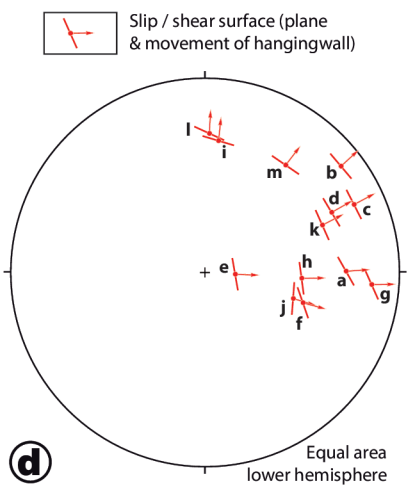

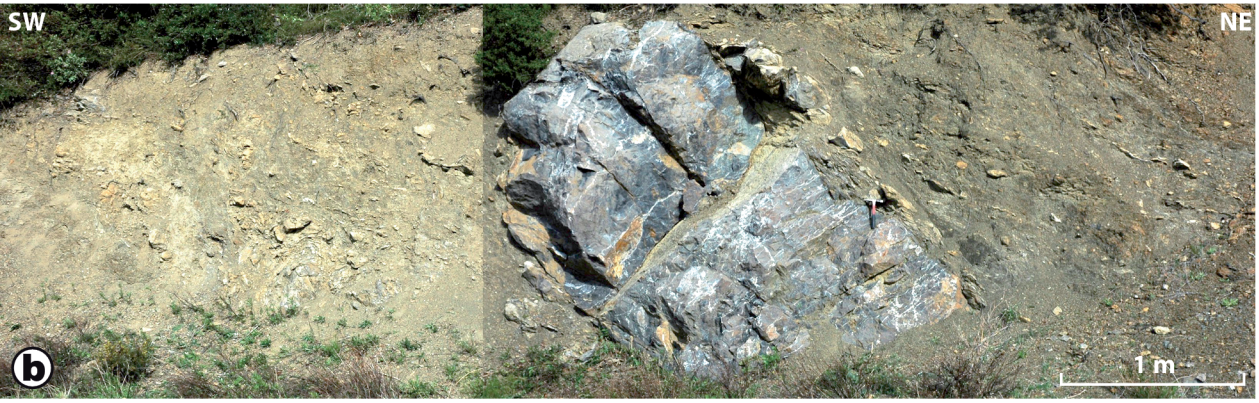

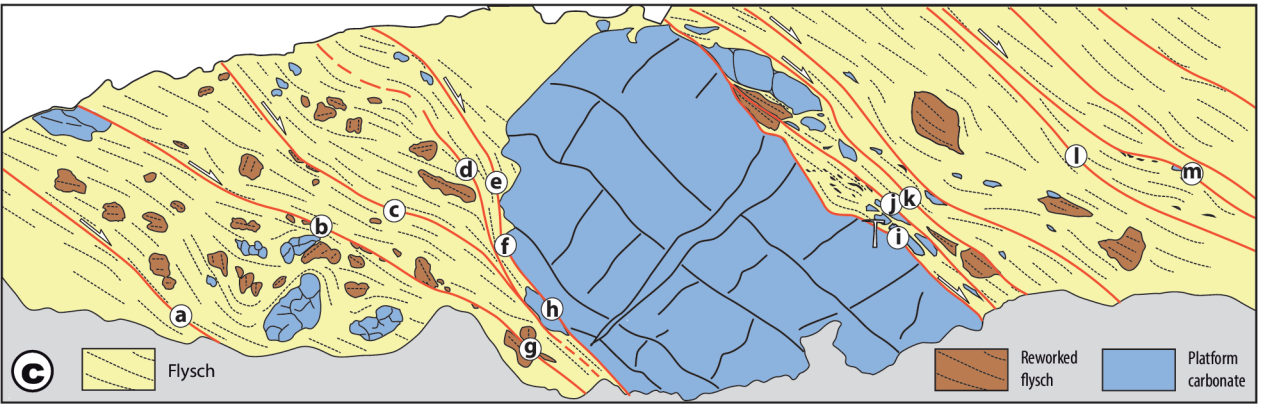

Chardon et al., Fig. 7 (1.5 column)

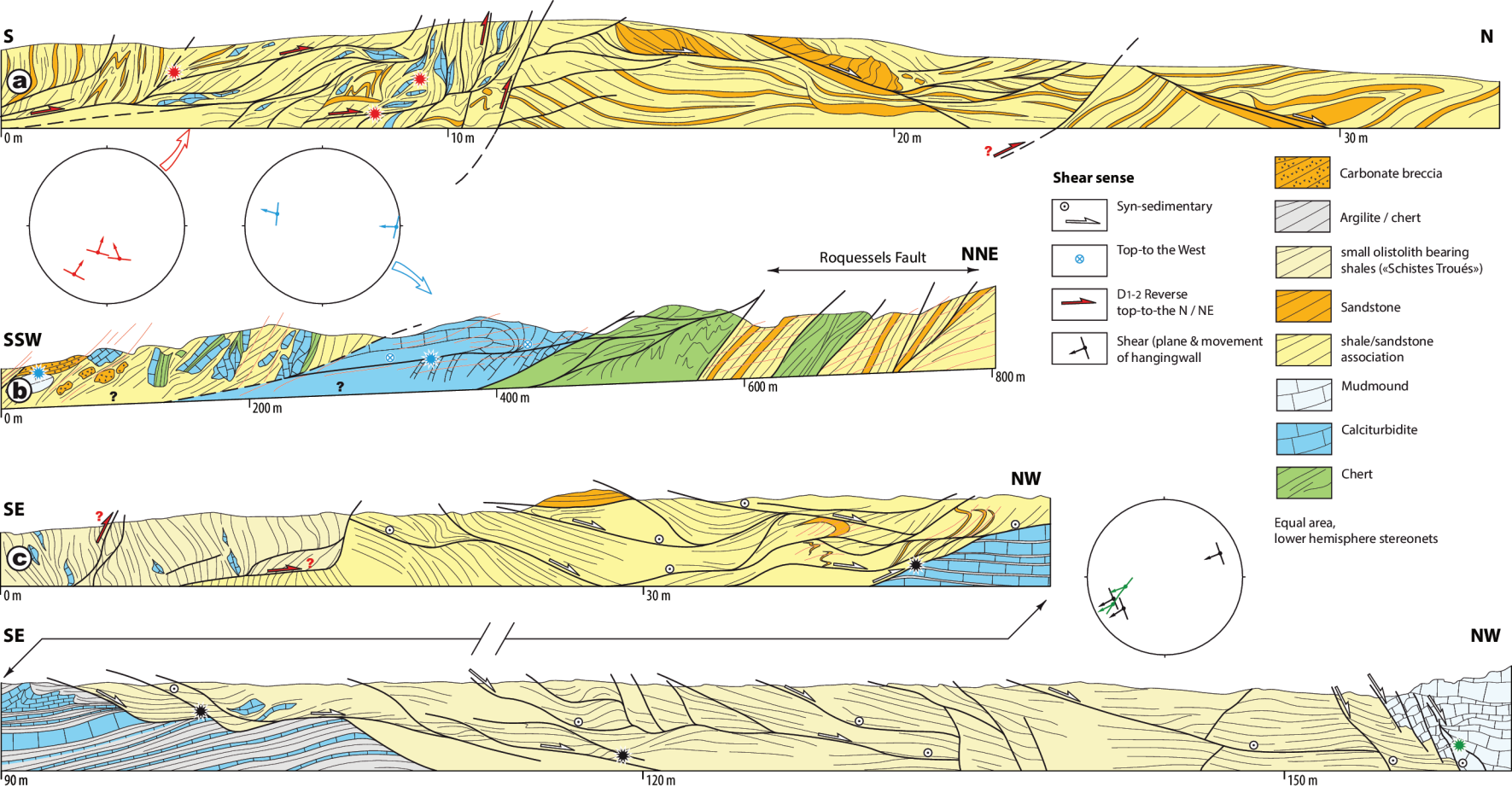

Chardon et al., Fig. 8. Full page, landscape orientation

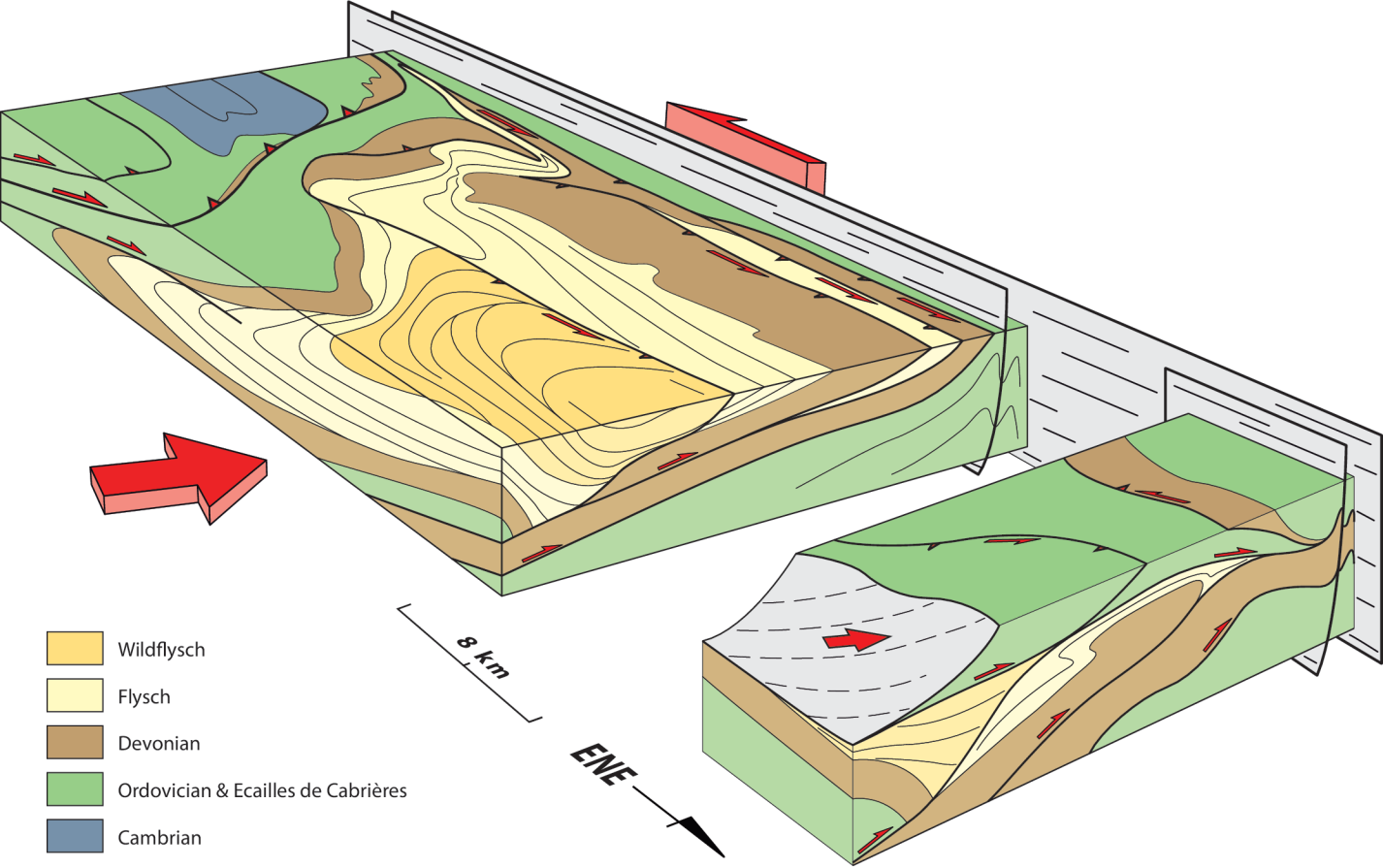

Chardon et al., Fig 9 (1.5 column)

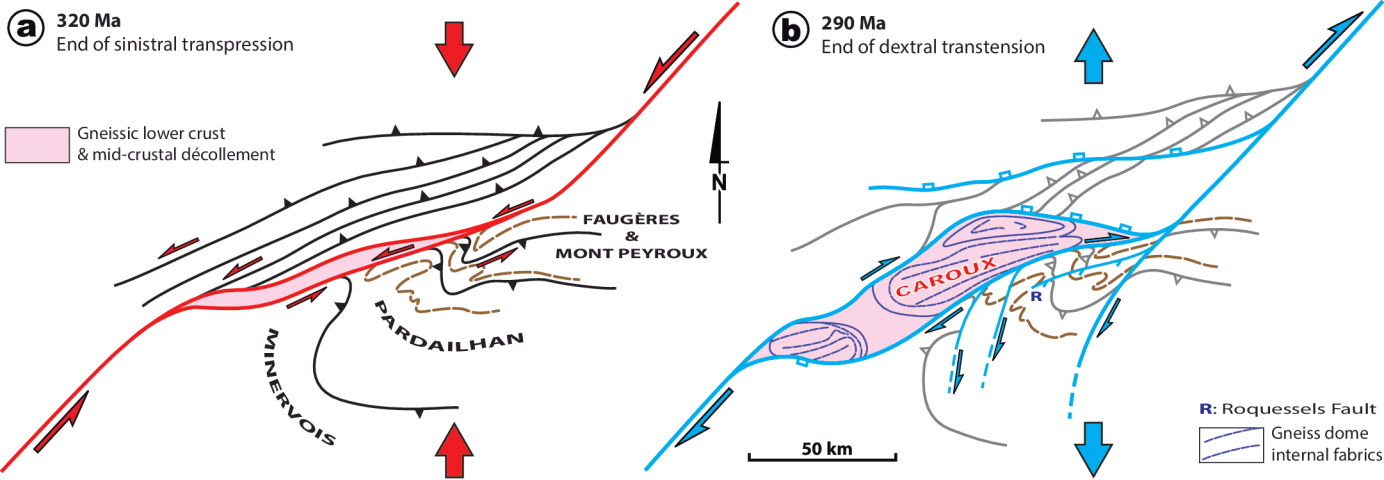

Chardon et al., Fig. 10 (2 columns)

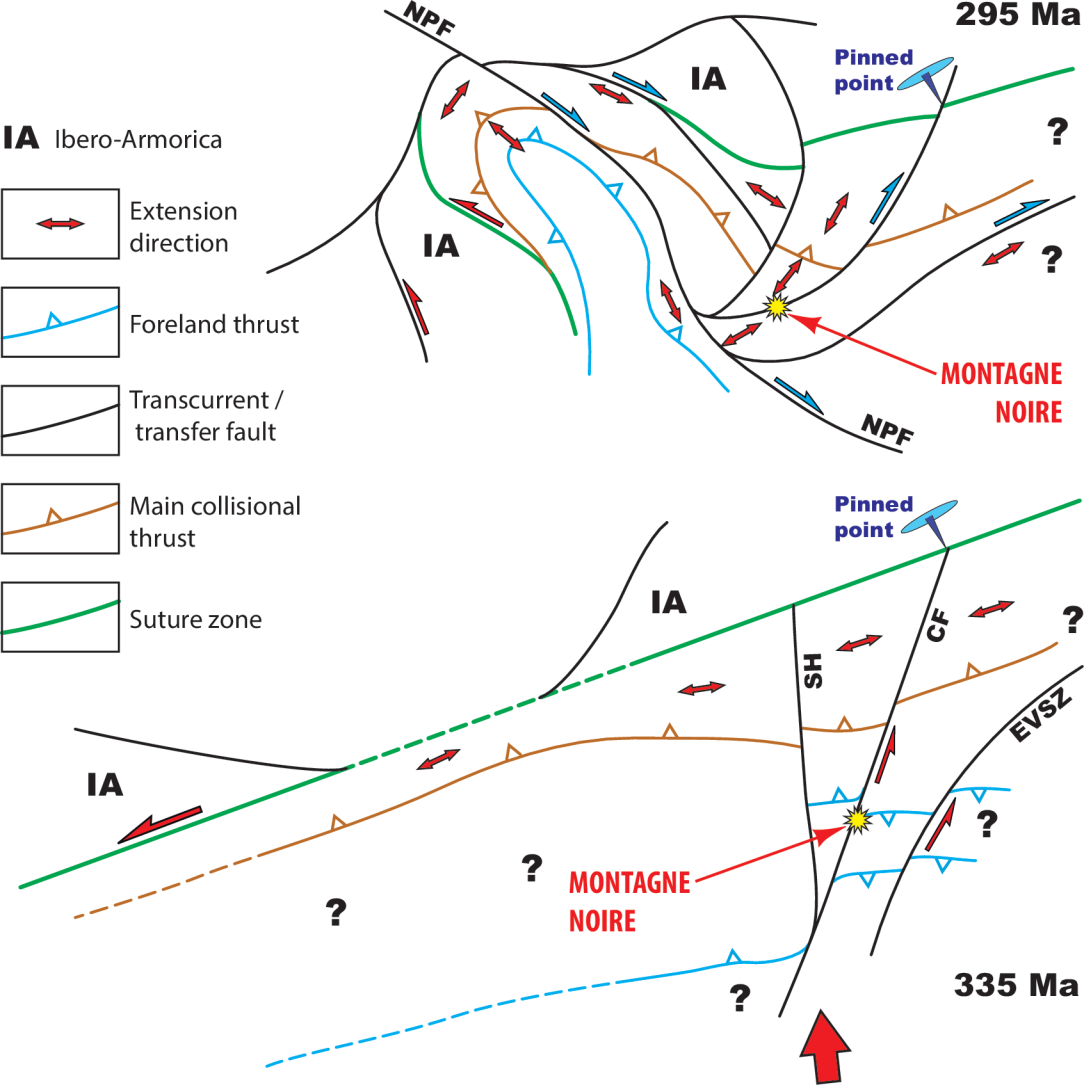

Chardon et al., Fig. 11 (1.5 column)

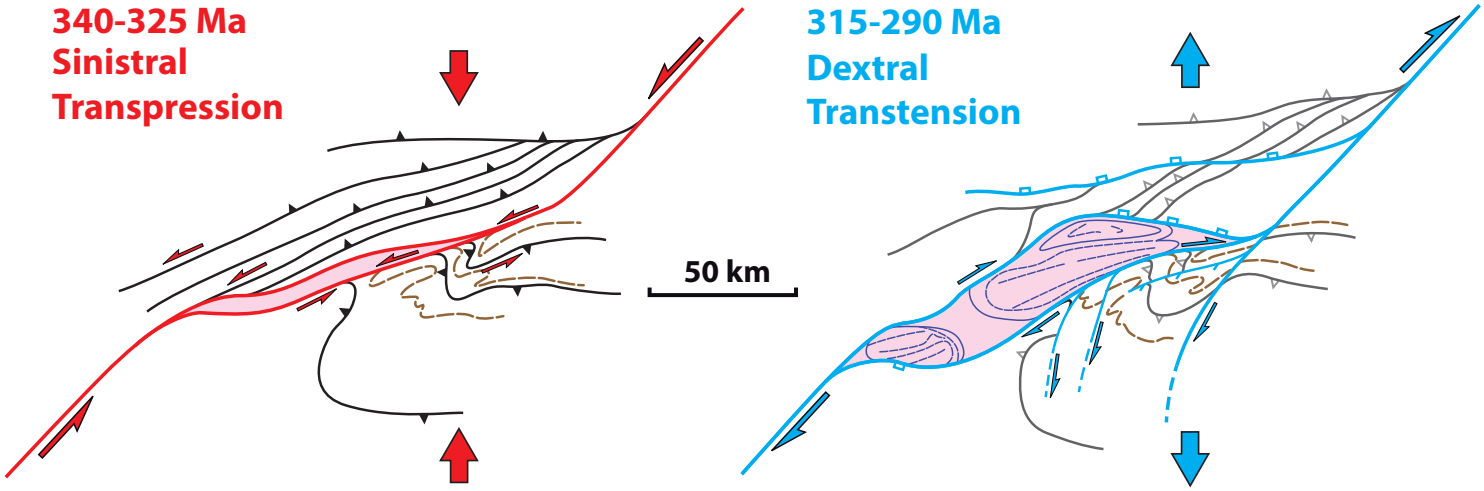

INVERSION OF THE CÉVENNES FAULT BEND, MONTAGNE NOIRE, SOUTHERN FRANCE